

UNIVERSITÀ DEGLI STUDI DELLA CALABRIA
Bernardino Telesio - Doctorate School of Science and Technique

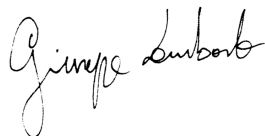
Doctorate curriculum in Mesophases and Molecular Materials

Scientific sector: FIS/07
XXIV Cycle

**Optical systems for diagnostics:
Near-Infrared Imaging technique for
detection of dental demineralisation**

Supervisors:

Dr. Giuseppe Lombardo



Dr. Christian Zakian



Curriculum Coordinator:

Prof. Carlo Versace



Phd Candidate:

Silvia Salsone



School Director:

Prof. Roberto Bartolino



To Giuseppe.

Abstract

In dentistry, a correct detection of caries severity is still a challenging decision-making task that crucially affects the choice for the best treatment plan. The challenge is to find both the most objective parameters to detect caries at different stages (from an early reversible stage to a severe one) and the most reliable method(s) that should be used to distinguish these stages. Currently, methods used in clinics are visual inspection, aided with light probe and pick inspection tools, and radiography. The main issue arising by the use of these methods is that both of them are subjective, with possibility for intra- and inter-examiner variability. For this reason, radiography needs an extreme care of interpretation especially when assessing occlusal caries. Visual methods, instead, are affected by confounding factors, such as stain or fluorosis, affecting the accurate assessment of early caries lesions. Radiography, moreover, should be performed with care considering that the emission of ionising radiation may cause malignant change in tissues, especially for young age patients and are counter-indicated during pregnancy. They are also inadequate for the detection of initial caries and to locate the lesions looking at the superimposition of the tooth along its buccal-lingual axis. The aim of this study was to overcome the limits of the current detection techniques, offering a non-invasive, objective method for the detection of caries at any stage of the demineralisation process. The proposed method measures the near-infrared (NIR) reflectance response of the tooth at three specific wavelengths. It is then possible to investigate properties of the sample at the surface and in depth and get an image that maps the lesions on the occlusal view of the sample when combining these wavelengths. Due to the properties of the NIR light, this method is non-invasive, non-contact and allows for detection both at the enamel and at the dentine level. The NIR method offers objective supporting information to quantify and detect dental caries and is especially suitable for areas affected by confounding factors, such as stain. The objective of the study was to design and implement a NIR

multispectral imaging system, developing efficient image analysis algorithms. In order to prove this objective, an in vitro validation of the technique against gold standard histology was performed together with a comparison to other detection methods - International Caries Detection and Assessment System (ICDAS - clinical visual inspection), fibre optic transillumination method (FOTI - visual inspection with light probe), radiography and Quantitative Light-induced Fluorescence method (QLF), used in clinics or in research. A total of 112 teeth, molars and premolars, with different lesion severities were used for this study. Histological sections were obtained to confirm the lesion severities and used as a gold standard to compare the sensitivity and specificity among techniques. Visual inspection methods recorded the highest values of sensitivity (ICDAS: >99%, FOTI: 93%) and specificity to dental caries (FOTI: >99%, ICDAS: 90%). However, these methods could have been highly facilitated by the in-vitro viewing of the samples. Sensitivity to dental caries was higher for NIR (91%) than for QLF (88%) and radiography (63%) while specificity was higher for radiography (81%) than for NIR (73%) and QLF (63%). The results from this study suggest that the NIR method has the ability to detect dental caries when other methods fail, providing an alternative to assist in the decision-making process with the further advantage of removing the confounding effect of stain. This method can enhance patient communication and offers an objective and safe alternative to ionising radiation methods.

Acknowledgements

I would like to thank Christian Zakian, who shared with me his knowledge, his work and his incredible passion for science and research; Giuseppe Lombardo, who always supported my path, in Italy and abroad, with intelligence and professionalism. Thanks to Pin Chew, my reference dentist, for her friendship and amazing way of teaching, who gave an important input to my work. Thanks also to Shelon, Juliana, Naveen, Andrew, who shared work and lab life always with a welcoming smile. Thanks to Maureen, Brenda and Arnold, Brian Daber and Angela Carson and her team at the Dental Hospital. A special mention to Prof. Keith Horner for the time dedicated to the project always with fun. Thanks for their patience, skills and hard work to the teams of the mechanical workshops both at the University of Calabria and Manchester.

I would also like to thank my friends, those who have been for ever and those who I met in the precious experience in Manchester and are now for ever friends. A very special thanks to my supportive colleagues in Milan, who encouraged me everyday, especially in the hard days. Thanks to Enrico for his lovely arts.

Thanks to my family, Giuseppe, who took an important part in this thesis with his patience, his support, his smartness and his contagious mood. Grazie a mia madre e mio padre, per il loro amore sempre presente. Grazie per appoggiare e sostenere le mie scelte, anche quelle difficili, e darmi la forza e il conforto anche a qualche migliaio di chilometri di distanza. Grazie alle mie nonne, che sento sempre parte di me, come Robi, per cui ho sempre un pensiero speciale.

Publications

S. Salsone, A. Taylor, J. Gomez, I. Pretty, R. Ellwood, M. Dickinson, G. Lombardo, and C. Zakian (2012) **Histological validation of near-infrared reflectance multispectral imaging technique for caries detection and quantification**, *J. Biomed. Opt.* 17(7), 076009

S. Salsone, P. Chew, J. Gomez, K. Horner, I. Pretty, R. Ellwood, M. Dickinson, G. Lombardo, and C. Zakian (2012) **Comparison of NIR Reflectance Multispectral Imaging Technique with Conventional Caries Detection Methods**, *Journal of Dentistry* (submitted)

Conferences and Poster presentation

CIMST Interdisciplinary Summer School on Bio-medical Imaging, ETH Zurich: *Near Infra-Red Imaging Technique for Early Tooth Decay Detection*

58th ORCA Congress (European Organisation for Caries Research), Kauanas: *Near Infra-Red Imaging Technique for Early Dental Caries Detection: An in-vitro comparison with ICDAS clinical scoring system* (poster and presentation, Abstract published on Caries Research Journal)

Optical Techniques in Clinical Practice, Institute of Physics Conference, London: *NIR multispectral reflectance imaging of teeth for caries visualisation as an alternative to x-rays* (poster and presentation) Biomedical Imaging Institute Showcase, University of Manchester: *Near Infra-Red Imaging Technique for Tooth Decay Detection*

Contents

Abstract	iii
Acknowledgements	v
Publications	vi
Conferences and Poster presentation	vi
List of Figures	x
List of Tables	xiii
1 Introduction: from Needs to Solutions	1
1.1 Dental caries	2
1.2 Methods for caries detection	5
2 Current State of the Art in Dental Caries Detection	9
2.1 Introduction	9
2.2 Internation Caries Detection and Assessment System	10
2.3 Fibre-Optic Transillumination	13
2.4 Quantitative Light-induced Fluorescence	14
2.4.1 Near-Infrared Fluorescence	16
2.5 Radiography	18
2.6 Electronic Caries Monitor	22

2.7	Near Infrared Transillumination and OCT	24
3	Histological validation of NIR reflectance multispectral imaging technique for caries detection and quantification	29
3.1	Introduction	29
3.2	Description of the technique	30
3.3	Materials and Methods	34
3.3.1	Sample Preparation	34
3.3.2	Instrumentation	36
3.3.3	Measurement Methodology	37
3.3.4	Histology	37
3.3.5	Image Analysis	38
3.3.6	Statistical Analysis	41
3.4	Results	42
3.5	Discussion	48
3.6	Conclusions	55
4	Comparison of NIR Reflectance Multispectral Imaging Technique with Conventional Caries Detection Methods	56
4.1	Introduction	56
4.2	Materials and Methods	57
4.2.1	Sample preparation	57
4.2.2	Description of the implemented methods	58
4.2.3	Histology	60
4.2.4	Statistical analysis	61
4.3	Results	62
4.4	Discussion	67
4.5	Conclusions	76
5	Conclusions	77
5.1	Summary and conclusions	77

5.2	Future work	81
5.2.1	LED experiment	82
5.2.2	Imaging fiber optic experiment	85

List of Figures

1	Illustration of a tooth section affected by caries and illuminated by NIR light.	xv
1.1	Caries World map from the WHO Report 2003.	2
1.2	Sectional view of the dental structure.	3
1.3	Tooth section with caries at the EDJ	5
2.1	Pictures of QLF light path[1]	15
2.2	DIAGNOdent system.	17
2.3	Configurations of dental intraoral radiography for caries detection.	19
2.4	Example of overlap on a bitewing radiograph.	21
2.5	Electrical Caries Monitor system.	22
2.6	Examples of mild fluorosis and MIH.	23
2.7	Example of NIR transillumination image of an enamel occlusal demineralisation.	25
2.8	Example of NIR transillumination image of a dentine occlusal demineralisation.	26
2.9	Example of PS-OCT image of a proximal demineralisation.	27
3.1	NIR hyperspectral imaging system.	30
3.2	Example of reflectance response curves from 1000 to 2500 nm of an occlusal tooth surface.	31
3.3	NIR hyperspectral imaging: selection of spectral images.	32

3.4	Illustration of a tooth section affected by caries and illuminated by NIR light.	33
3.5	Examples of teeth with different carious lesions.	35
3.6	NIR multispectral imaging setup.	36
3.7	Example of a histological hemi-section.	38
3.8	Example of calibrated NIR polarised images.	39
3.9	Examples of NIR images for S_e and S_d	40
3.10	Examples of NIR images for S_{caries}	43
3.11	Boxplots of S_{caries} against histological scores.	44
3.12	Example of overscoring.	50
3.13	Examples of overscoring.	51
3.14	Example of underscoring.	52
3.15	Example of overscoring.	53
3.16	Examples of teeth affected by stain.	54
4.1	Colour image, histological section, X-rays, FOTI, QLF and NIR S_{caries} images of a sound tooth.	63
4.2	Colour image, histological section, X-rays, FOTI, QLF and NIR S_{caries} images of a tooth with enamel lesions.	63
4.3	Colour image, histological section, X-rays, FOTI, QLF and NIR S_{caries} images of a tooth with dentine lesions.	64
4.4	QLF technique: issues	70
4.5	Case of NIR S_{caries} over-scoring	70
4.6	Case of NIR S_{caries} under-scoring	71
4.7	Case of tooth affected by fluorosis.	73
4.8	Case of lesion NIR S_{caries} and Radiography are able to detect while other methods fail.	74
5.1	Comparison between NIR maps obtained with different light sources.	83
5.2	LED NIR reflectance images	84

5.3	LED NIR reflectance images with imaging fiber bundle	86
-----	--	----

List of Tables

2.1	ICDAS visual scoring system: classification of lesion severity.	11
2.2	ICDAS classification in relation with lesion histological depth.	12
2.3	FOTI visual scoring system: classification of lesion severity.	13
2.4	Radiography: classification of lesion severity.	20
2.5	ECM: classification of lesion severity.	24
3.1	Mean and standard deviation values.	43
3.2	Confidence table.	44
3.3	Values of thresholds, AUC, sensitivities, specificities, and Youden's indices at each lesion level.	45
3.4	Values of sensitivities and specificities at three lesion levels.	46
3.5	Sensitivity and specificity of S_{caries} at three lesion levels for the unpolarised experiment.	47
4.1	ICDAS, FOTI and Radiography scoring criteria.	58
4.2	Confidence table of the visible methods in comparison with histology at the three detection levels.	64
4.3	Confidence table of QLF, Radiography and NIR methods in comparison with histology at the three detection levels.	64
4.4	Results of visual methods in comparison with histology.	65
4.5	Results of QLF, Radiography and NIR methods in comparison with histology.	65

4.6	Values of sensitivity and specificity at the three detection levels for visual methods.	66
4.7	Values of sensitivity and specificity at the three detection levels for QLF, Radiography and NIR methods.	66
4.8	AUC accuracy at all the detection levels for the methods requiring ROC analysis.	66
4.9	values of Spearman's correlation at all the detection levels for all the methods.	67
4.10	Properties of the techniques.	74

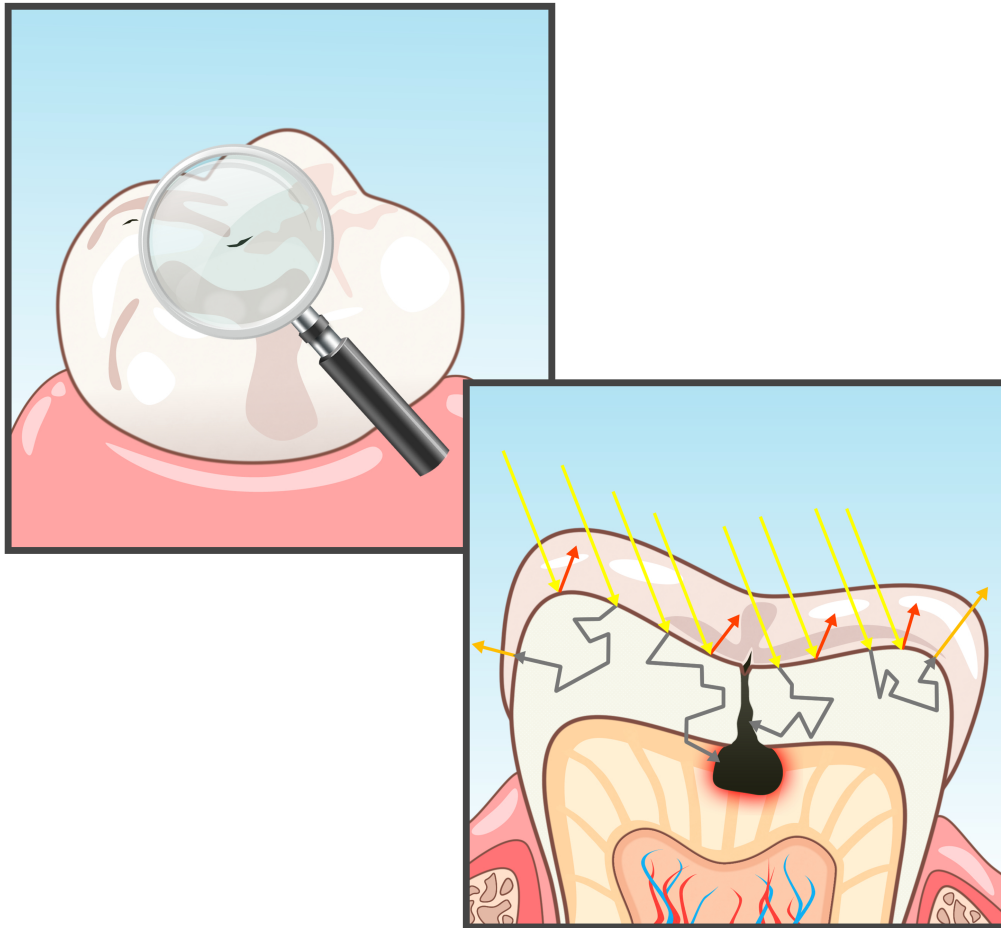


Figure 1: Illustration of a tooth section affected by caries and illuminated by NIR light. *Illustration courtesy of Dr. Enrico Garavaglia*

Chapter 1

Introduction: from Needs to Solutions

The spread of oral disease occurrences around the world (Figure 1.1) triggered off the inclusion of oral health plans as part of the policies for general health promotion.

The direction given by the World Health Organization (WHO) in the Oral Health Programme of the Department of Chronic Disease and Health Promotion is towards disease prevention. Oral diseases have a strong impact on quality of life, pain and malnutrition, and community spending. Dental caries is currently the fourth most expensive disease to treat[2]. Malnutrition, namely dietary excess in developed countries, is one of the main causes of dental caries. Sociocultural aspects, such as poor living conditions, low education level and social inequalities, are related to high risk of oral disease. The public and the governments still consider dental health as a secondary problem, while promoting healthy diet and hygiene would play a role also in the action against caries. Moreover, health payment systems should revert the well-established policy of supporting operative treatment costs only, engaging instead a preventive healthcare approach[3] that would improve people's quality of life and save community spending. Apart from appropriate diet

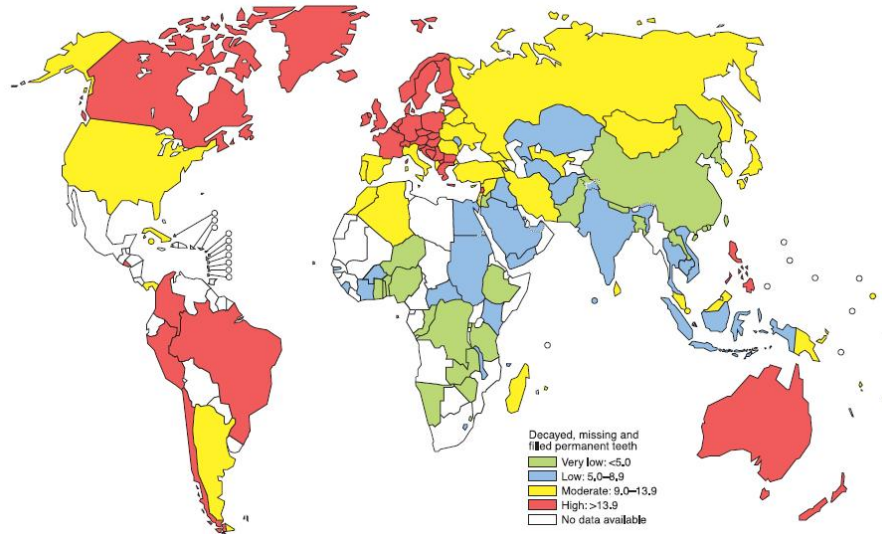


Figure 1.1: Caries World map from the WHO Report 2003.

and tooth cleaning procedures, preventive non-surgical therapies for caries include the use of fluoride as a remineralising agent and periodical visits allowing detection of early lesions and monitoring of their activity. At present, no gold standard of lesion activity in a single examination is available[4, 5].

1.1 Dental caries

Dental histology. Enamel is the outer layer of the tooth and is mainly constituted by minerals. During the enamel formation (amelogenesis), ameloblasts, cells responsible for the amelogenesis, secrete an organic matrix made of proteins that will later mineralise, expelling water and proteins and absorbing calcium and phosphate, to form the hard mature enamel. Enamel is structured in enamel prisms. These are rod-shaped structures of about $4\ \mu\text{m}$ in diameter where hydroxyapatite crystals are bound together. Interprismatic spaces divide and connect one prism to the other where the composition is made of the same crystals as inside the prisms but with different orientation,

resulting in a non-homogeneous material at a lower scale.

Dentine is the dental layer supporting the enamel and is less mineralised than enamel. During the formation of dentine (dentinogenesis), odontoblasts, cells responsible for the dentinogenesis, secrete collagen-rich organic matrices. These matrices consist of collagen and other proteins necessary for the following mineralisation process. The mature dentinal tissue is structured in closely packed tubules. In the outermost layer of dentine, called primary dentine, most of the collagen is contained.

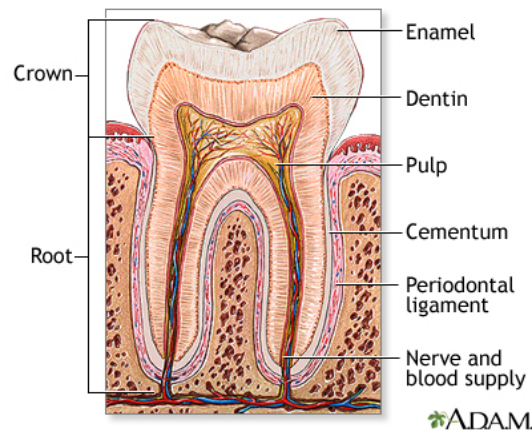


Figure 1.2: Sectional view of the dental structure.

Caries process. What constitutes dental caries is a community of organisms attached to a pellicle coating the dental tissues. This is a process starting with the formation of biofilm, foundation for dental plaque, when the dental tissue is exposed to water and nutrient. In biofilm, some bacteria metabolise carbohydrate producing organic acids while others metabolise amino acids producing ammonia, which is basic, and more bacteria[6, 7]. If these two processes are balanced, caries will not start. But if there is an excess of fermentable carbohydrate the pH of the plaque will decrease, reaching critical values for caries formation, namely about $\text{pH}=5$ [8]. This will lead to disso-

lution of dental minerals, namely hydroxyapatite, favouring the formation of a carious lesion. At the beginning this is known as white spot lesion due to the chulky appearance created by the mineral loss that increases the porosity of the enamel surface and so the refractive index gradient[6, 9].

Caries develops where the biofilm remains untouched by mechanical interactions with tongue, cheeks, abrasive food and toothbrushing for prolonged periods of time. Since the enamel prisms, described in the previous paragraph, are alined perpendicularly to the underlying dentine (Figure 1.2), the direction of the prism structure influences the shape of the white-spot lesions as well as the progression of the caries in depth through enamel. Moreover, unlike enamel, the inner layer of dentine continues its formation throughout life and odontoblasts can generate more odontoblasts if exposed to external stimuli such as caries progressing from enamel. If the stimuli are severe the odontoblast creation process will be rapid resulting in an irregular organisation of the new cells, while less severe stimuli will generate odontoblast tubular patterns. Dentine reacts to caries progression also by deposition of mineral within the dentinal tubules, blocking the tubules and slowing the bacterial attack. This process is called tubular sclerosis. This phenomenon starts before the enamel lesion reaches the enamel-dentine junction (EDJ), the borderline area between enamel and dentine. When the lesion comes into contact with the EDJ, a dark brown line at the EDJ is visible (Figure 1.3), indicating the extent of the enamel lesion contact area at the EDJ, and the demineralisation starts also in dentine causing the typical brownish v-shaped appearance (when seen in a longitudinal section of the tooth). At this stage, the appearance is not yet related to the spread of the lesion, since it never spreads laterally beyond the extent of the lesion at the EDJ. This reaction of the dental system is due to the presence of biofilm at the tooth surface, causing the transmission of a stimulus through the enamel prisms. This shows how the caries process is strongly related to the presence of bacteria on the biofilm and the acids present in the oral cavity, activating bacterial

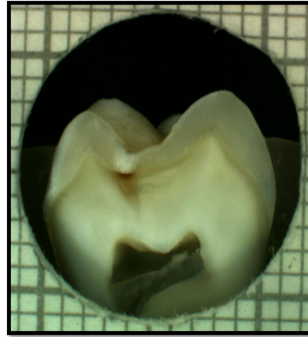


Figure 1.3: Example of longitudinal section with caries at the enamel-dentine junction (EDJ). The dark brown line indicates that the carious attack has reached the EDJ. The brownish discoloration at the dentine level is not yet due to demineralisation but to the reaction of the tissue.

metabolisms. Disturbing the biofilm formation will then prevent the process to start. Moreover, the lesion can be arrested at any stage of the caries process, no matter at which depth the tissue has been affected. This can be done by removing the biofilm, stopping mineral loss and allowing for mineral gain. Lesion activity is an important clinical knowledge in order for the dentist to make a decision on what kind of treatment to undertake, whether preventive/non-operative or operative[10]. As reported above, a standard detection system able to discriminate between active and arrested lesion in a single examination does not exist, despite research efforts[11, 12, 13].

1.2 Methods for caries detection

Objective methods for early detection, assessment, and monitoring of the disease are needed to allow the early implementation of therapeutic interventions and to monitor treatment outcomes. The ability to avoid the need for surgical intervention has benefits for both patients and social medicine service budgets[5].

Inherent limitations experienced by current methods are subjectivity[14,

15], single-point examination, the confounding factor of stain and undesired ionising radiation which render them unsuitable in various diagnostic scenarios. Visual inspection is routinely used by dental clinicians to detect and assess caries; however, this is a subjective measure and requires training. Clinical visual methods for caries detection and assessment have been improved to enhance the detection ability and reliability, especially of early lesions, such as the International Caries Detection and Assessment System (ICDAS)[16, 17] or the Nyvad score system[12, 13]. Traditional dental radiography is still the most widely used detection aid in dental practice but is inadequate for the detection of incipient demineralization since it can detect lesions when they are already advanced and surgical treatments may be necessary[14, 18, 19]. A high inter- and intra-observer variability makes the diagnosis challenging and the detection of occlusal fissure lesions requires care in interpretation, producing both false positive and false negative results otherwise[20]. Dental radiographs also carry a small risk of inducing malignant change in tissues and this is an important issue when frequent radiographs are required in particular with younger age groups.

New technologies for assisting clinical decisions as well as for rendering the detection more objective have been studied. Fiber-optic transillumination, based on visual inspection with the aid of a white light probe, have been used as detection aids to visualise the internal contrast between sound and decayed regions within teeth[14, 21], but these do not allow an absolute quantification of lesions due to the heterogeneous light distribution within the tooth. Caries quantification methods based on electrical tooth impedance measurement (ECM)[22, 23] and bacterial fluorescence related to dental caries (DIAGNOdent)[24, 25] have been also reported, but these only provide single point measurements and do not allow visualization of the lesion distribution. Such single point measurements are prone to errors, especially when longitudinally monitoring lesions, as it can be difficult to achieve iden-

tical repositioning between patient visits. Imaging methods based on the loss of natural light fluorescence in teeth as a result of light scattering in porous tissue, such as quantitative light fluorescence (QLF)[26, 27], have shown the ability to detect and quantify lesions. Optical methods are, however, affected by the presence of stain on teeth (especially occlusal surfaces) as it absorbs visible light, and some care is required in the interpretation of images.

The use of near-infrared (NIR) wavelengths has been explored as they show little absorption by stain and have a deeper penetration in teeth (the mean free path of the photons being ~ 3 mm at 1310 and 1550 nm, while under 0.1 mm for visible wavelengths)[9, 28, 29]. NIR transillumination imaging[30] has been shown to enhance lesion contrast visualization; in particular, quantification of lesion based on image contrast was used with line profile drawing and pre-knowledge on sound areas. Moreover, 1310-nm (NIR) wavelength optical coherence tomography (OCT) has been investigated as a possible method to measure backscattered light intensity in relation to dental porosity and provide cross-sectional structural information from the surface and sub-surface of teeth[31, 32, 33]. A recent study has demonstrated that NIR spectral imaging can be used to quantify and map lesion distribution and severity at both enamel and dentine levels[19]. Although the results were promising, this was an explorative study using hyperspectral imaging to find characteristic wavelengths for quantitative analysis, which would be impractical for use in the mouth. Moreover, specular reflections associated with tooth morphology impeded detection and cross-polarization has shown to remove their effect[34]. The aim of the current study is a) to simplify the optical design of that study and explore NIR cross-polarised multispectral reflectance imaging to remove specular reflections; b) to validate the sensitivity and specificity of the quantitative detection method using a combination of key wavelengths, allowing for automatic lesion detection without the need of user input, in an in vitro study against a histological reference standard;

and c) to compare the NIR reflectance to the conventional detection methods and to techniques that are currently used in research, namely visual methods such as ICDAS and FOTI, radiography and QLF. This was carried out on the same sample set to allow for a direct comparison. The comparison was qualitative and quantitative, looking at different features of the techniques mentioned above and at the sensitivity and specificity of occlusal caries detection for each method.

Clinical examinations were performed for this research by Prof. Roger Ellwood and PhD student Juliana Gomez; radiograph examination was performed by Prof. Keith Horner and Dr. Pin Hooi Chew.

A background of these techniques implemented during the comparative phase of the project are described in Chapter 1, with an overview on the clinical visual methods and technical details on the methods currently investigated by the research arena.

The development of the NIR reflectance method from the hyperspectral system to the multispectral system is shown in Chapter 2, with a description of the sample preparation, the measurements methodology, the image analysis, the description of the method of validation through histological hemi-sections and the results discussion in terms of sensitivity and specificity statistical analysis.

In Chapter 3 the comparison of the NIR reflectance method to other caries detection methods is presented, showing how these methods together with histology were implemented, and the performance of each technique is quantitatively and qualitatively compared.

Finally, concluding remarks of this thesis and some comments on possible future directions can be found in the Conclusions section.

Chapter 2

Current State of the Art in Dental Caries Detection

2.1 Introduction

This chapter gives an overview of some of the techniques currently used in both clinics and the research environment. In particular, the focus of this review is on techniques that are in a development phase either at the laboratory stage or being employed in clinical trials. Each of these techniques has its advantages and disadvantages that when combined help the dental clinician to investigate about different aspects of the tooth and allow for an informed diagnosis.

Detection techniques assess lesion severity based on either a visual or non-visual scoring system. The former requires visual abilities and to follow defined inspection criteria in order to yield a score; the latter produces either a score or an image by means of a technical device. Digital diagnostic techniques belong to this category. Visual scoring systems are subjective and prone to intra- and inter-examiner variability. Reducing this is a key objective when developing these methods. The main issue being that they are based on variation of sample colour and colour discrimination, which

may not be an absolute parameter for anyone as well as for each person at different times. Visual methods hardly discriminate between deep enamel and shallow dentine lesions[18, 35]. Non-visual scoring system may be more objective but they may be affected by some degree of subjectivity if they need user input or background knowledge to be used.

Another possible classification is between imaging method and non-imaging method. The former is characterised by the output of an image of diagnostic relevance and belongs to the non-visual system category; visual and digital single-point scoring systems belong to the latter. Imaging methods have many advantages, such as the possibility of freezing favourite views of the sample, zooming-in interested areas if the image quality allows for it, involving to some degree the patient in the examination procedure in order to enhance dentist-patient communication, filing examination results at different visits and comparing images of the same sample at different time-points for disease monitoring purpose. Single-point measurement methods allow for an indication of the extent of the disease but with no possibility to spot any area where the disease is affecting the sample nor to repeat the same measurement on different examination times, therefore it cannot discriminate between a change due to the different measurement and a modification in the tissue.

2.2 Internation Caries Detection and Assessment System

Internation Caries Detection and Assessment System (ICDAS) is a visual scoring system that provides a coding classification related to the appearance of the tooth, as shown in Table 2.1[16, 17].

Each score has an associated histological value, based on a validation study[36], giving to each score a relation to the actual severity of demineralisation. The relationship between ICDAS scores 0-6 and histological depth is presented in Table 2.2. There are several studies involving ICDAS, con-

ICDAS score	Definition
0	Sound tooth surface: no evidence of caries after prolonged air drying (5 s)
1	First visual change in enamel: opacity or discoloration (white or brown) is visible at the entrance to the pit or fissure after prolonged air drying, which is not or hardly seen on a wet surface
2	Distinct visual change in enamel: opacity or discoloration distinctly visible at the entrance to the pit and fissure when wet, lesion must still be visible when dry
3	Localized enamel breakdown due to caries with no visible dentine or underlying shadow: opacity or discoloration wider than the natural fissure/fossa when wet and after prolonged air drying
4	Underlying dark shadow from dentine \pm localised enamel breakdown
5	Distinct cavity with visible dentine: visual evidence of demineralisation and dentine exposed
6	Extensive distinct cavity with visible dentine and more than half of the surface involved

Table 2.1: ICDAS visual scoring system: classification of lesion severity.

sidered as the reference visual scoring system[37, 38, 3, 39], in many review studies and comparative studies[15, 40, 41, 42].

The ICDAS system requires the cleaning of teeth prior to examination to aid detection, as many other visual and non-visual systems, since caries forms where plaque stagnation is present. In addition, the use of compressed air is necessary to reveal the earliest visual signs of caries, due to the porosity of the surface. The lesion that is visible only on a dry tooth surface is probably in the outer enamel, whereas a lesion visible on a wet tooth surface has penetrated the enamel and maybe reached the dentin. Enamel’s refractive index is 1.62, on average in the visible range. The difference between the enamel’s refractive index and saliva, supposing having a refractive index similar to water, 1.33 on average for visible wavelengths, is smaller than the air’s one when the surface is dried with the use of compressed air[6]. Moreover, a porous dry surface scatters more light than the same wet surface, so water makes the enamel look brighter and smoother, while in a dry porous enamel early lesions look chulky and therefore are highlighted.

ICDAS score	Histological depth
0	No enamel demineralization or a narrow surface zone of opacity (edge phenomenon)
1	Enamel demineralization limited to the outer half of the enamel layer
2	Demineralization involving between half of the enamel and the outer third of the dentine
3	Demineralization involving the middle third of the dentine, clinically microcavitated...complete description
4 (3)	Demineralization involving the middle third of the dentine, clinically shadowed
5 (4)	Demineralization involving the inner third of dentine \pm into the pulp, clinically cavitated but the cavitation covers less than half of the surface
6 (4)	Demineralization involving the inner third of dentine \pm into the pulp, clinically cavitated but the cavitation covers more than half of the surface

Table 2.2: ICDAS classification in relation with lesion histological depth.

Table 2.2 should help the examiner to decipher tooth appearance into actual level of demineralisation. Unfortunately, as the difference between consecutive scores is negligible and subjective, this method is effective at distinguish between sound and non-sound cases but a sensitive assessment of caries severity is hard to perform. ICDAS score 1, 2 and 3 are related to very little changes of appearance on the tooth so early detection results difficult. Training and experience are important requirements for an ICDAS examiner. Moreover, while score 1 should represent demineralisation limited to the enamel, score 2 and 3 should involve also dentine, as indicated by Table 2.2, in fact in contrast with the description of the score, indicating demineralisation evidence on the enamel only. So, on one hand, these are big obstacles for early detection; on the other hand, dentine caries assessment and detection also results to be difficult due to stain confounding effects. Stain can be easily mistaken for caries because often covering areas where normally caries attacks take place, on the occlusal fissures. The opposite confounding effect could also happen since tooth stain could hide a lesion

whose depth would be therefore impossible to assess.

2.3 Fibre-Optic Transillumination

Fibre-Optic Transillumination (FOTI)[43] is a caries detection tool used to implement an aided visual scoring method. Typically, the FOTI equipment has a fibre-delivered illumination source (Schott Fibre Optics, Doncaster, UK) with a halogen lamp (150 W), connected to an optical fibre that brings the light to the 0.5 mm tip of a dental probe. The visual inspection with the aid of the probe is enhanced by placing the tip of the probe at the cemento-enamel junction perpendicular to the buccal and lingual surfaces and scanning along the surface. The appearance of tooth defects improves due to the transparency of the enamel that allows for the fluorescence of the transilluminated dentine to appear at yellow/orange wavelengths. The overall look of the tooth is yellow when sound, with dark areas where there are enamel demineralisations or stain, which impede light scattering to pass reaching the observer, while orange shadows appear in presence of affected dentine. FOTI score classification is shown in Table 2.3.

FOTI score	Definition
0	No shadow or stained area
1	Lesion stays the same width when transilluminated/Thin grey shadow into enamel when transilluminated
2	Wide grey shadow into enamel when transilluminated
3	Wide grey shadow into enamel with no evidence of dentine shadow
4	Orange/brown or bluish/black shadow < 2mm in width
5	Shadow as described above and/or transillumination light is blocked > 2mm in width
6	Large area of frank cavitation with likely pulpal involvement

Table 2.3: FOTI visual scoring system: classification of lesion severity.

In use since the 70s, it was developed as an alternative technique other than bitewing radiographs for the diagnosis of caries in clinical trials, since

it had the ability to enhance visual inspection. It was found that it might considerably increase visual detection and it was largely used in many comparative studies and clinical trials[14, 23, 44, 18, 35, 40]. More recently it spread as detection tool in clinical practices. As all visual systems, FOTI is affected by subjectivity, intra- and inter-examiner variability, longitudinal monitoring is not an easy task and training is required in order to be competent at using FOTI. An imaging version of FOTI has been developed, digital imaging FOTI (DIFOTI). DIFOTI is made of a high intensity light and grey scale camera which can be configured for smooth and for occlusal surfaces. Images can be produced, visualised and archived for retrieval at a repeat visit. However, there is no attempt within the software to quantify the images, and analysis is still undertaken visually by the examiner who give a score subjectively based on the appearance of scattering[21, 8].

2.4 Quantitative Light-induced Fluorescence

Quantitative Light-induced Fluorescence (QLF) is a laser fluorescence method for caries lesion assessment based on fluorescence changes in presence of caries. Light in the blue-green region is used to induce natural yellow and red fluorescence of enamel. Enamel demineralisations reduce this fluorescence, so QLF correlates fluorescence loss to carious lesions.

The source of the auto-fluorescence is thought to be at the enamel dentinal junction, while the transparent enamel makes the fluorophores contained within the EDJ to pass through[8]. In a first implementation of the QLF method by Bjelkhagen[45] the tooth was illuminated with a blue-green light from an argon ion laser at $\lambda=488$ nm and a yellow high-pass filter, cutting off light scattered with a lower wavelength than 520 nm, made the yellow/red fluorescence from the enamel to be observed. This device, which could be used for in vitro measurements only, was followed by technical improvements, such as a probe with an intra-oral camera for in vivo measurements and the

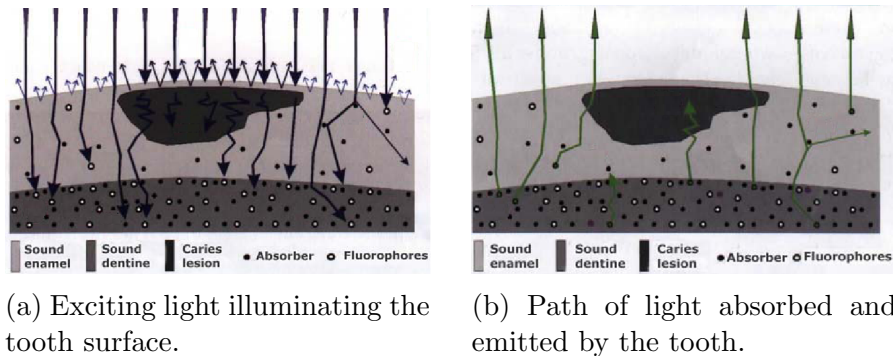


Figure 2.1: Pictures of QLF light path[1]

use of xenon lamps in the blue spectrum instead of the argon ion laser, as well as the creation of a software for in vivo examinations.

It is not clear which are the responsible chromophores causing the tooth fluorescence and neither the mechanism behind the fluorescence loss in presence of caries. The generally accepted explanation is that light scattering in the lesion, being stronger than in sound enamel, causes a shorter light path than in sound enamel (Figure 2.1a). Another possible explanation, which may contribute to the first one, is that the fluorescence is due to the collagen present in dentine and that the enamel lesion behaves like a barrier so that the exciting light is scattered by the lesion and cannot reach the underlying fluorescing dentine (Figure 2.1b); at the same time it is a barrier for the fluorescence light from dentine to reach the surface[46, 47, 1]. The analysis algorithm[48] firstly consists of the creation of a baseline image, where the image of the examined tooth is reconstructed simulating it as sound, based on a rectangular mask the user has to draw around the lesion. The algorithm assumes the mask lines are drawn over sound tissue and interpolates the observed sound enamel fluorescence values on the mask circumscribing the lesion. This is to construct corresponding *sound* fluorescence values inside the mask, thus at the lesion site. Then, the difference between the baseline reconstructed *sound* image and the actual image is calculated, yielding fluorescence decrease as a function of position (x, y) on the tooth surface at the

location of the lesion, expressed as a percentage of the fluorescence in the sound situation:

$$\Delta L(x, y) = \frac{L_{sound}(x, y) - L_{cariou}(x, y)}{L_{sound}(x, y)}$$

Once values of fluorescence decrease are obtained, three quantities are calculated: ΔL_{max} , *Area* and ΔL_{mean} . ΔL_{max} is the maximum value of $\Delta L(x, y)$ in a lesion; *Area* is the lesion area, usually defined as the area where the loss of fluorescence is $> 5\%$ of the value of sound tissue; and ΔL_{mean} is the mean value of $\Delta L(x, y)$ over that area. The software for subtraction and evaluation is usually custom-developed either by the user or the manufacturer Inspektor Research Systems (Amsterdam, the Netherlands).

One of the issues of this method is that user input is required in order to perform the analysis algorithm and get a score. This means the operator needs training for instrument use and accurate knowledge of caries processes in order to assess which lesion area to investigate, what can be considered as sound tissue on each image, what kind of mask to draw in case of lesion monitoring, since the same mask is used by the algorithm for future repeated evaluations in order to be comparable. Moreover, the result consists of quantities related only to the investigated lesion, such as demineralisation area, maximum and mean fluorescence loss, even though a fluorescence image of the whole tooth is also returned. No discrimination between fluorescence loss due to caries and to stain is possible.

2.4.1 Near-Infrared Fluorescence

Thylstrup et al.[46] could not report about a red-light induced fluorescence since at the time fluorescence studies had not yet revealed any visible fluorescence due to illumination at 633 nm while it was well-known that blue light induced enamel and dentine fluorescence in the visible spectra. Fluorescence intensity decreases when demineralisation occurs, so mineral loss can

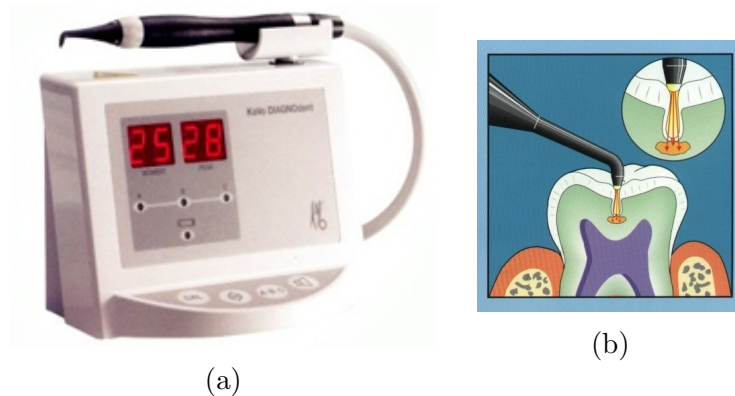


Figure 2.2: DIAGNOdent: (a) the laser fluorescence device and (b) the principle.

be estimated, as reported in section 2.4. Only more than 10 years later it was discovered that red light (638-655 nm) induced an infra-red fluorescence that allowed for discrimination between sound and carious tissue[49]. Fluorescence yield decreases with increasing wavelength, but this phenomenon is more relevant for sound tissue compared to demineralised enamel or dentine. Then, presence of caries causes increases of fluorescence intensity to be registered[50].

The system consists of a modulated diode laser at 655 nm to separate fluorescence from long wavelength light, a long pass filter, which cuts off the excitation light and other short wavelength light, and a photo-diode detector. The principle behind the enhanced fluorescence in the presence of caries is not clear yet but a proposed hypothesis is that proto- and meso-porphyrins, bacterial metabolites from the mitochondria respiratory chain, may be responsible for this fluorescence variation[51, 52].

This instrument reached the market with the name of DIAGNOdent (Figure 2.2) and several studies and review works investigated and evaluated its abilities[8, 25, 53, 40, 54].

Limitations of this instrument may be presence of plaque, calculus, staining on the tooth surface, the degree of dehydration of tooth tissue, the

position of the tip, which needs to be tilted forwards and back in the fissure for all surfaces to be scanned. Most of these confounder factors tend to cause an increase in the output reading, leading to false-positives. Moreover, the output of this technique is made of two numbers, the first displaying the current reading while the second displaying the peak of the examination, with no possibility of lesion location.

2.5 Radiography

Radiography is still one of the most common diagnosis aids in dental practice. It has been showed it improves the diagnosis of approximal caries, clinically undetected dentine caries[55, 56], also known as “hidden caries” where dental surface clinically looks intact while a lesion spreads in dentine, and dentinal demineralisations in general[57, 58]. One of the main objections to this method is that it is not efficient at detecting occlusal lesions, especially at the enamel[19]. The main cause of the difficulties at detecting occlusal lesions is related to the output of radiography, namely the two- dimensional projection in the buccal-lingual direction of a three dimensional object. It is, therefore, difficult to locate the site where a lesion starts and develops on the occlusal enamel, considering this is flatten on the radiograph. Moreover, it may also happen that the lesion is hidden by sound enamel tissue or by dentinal tissue, due to a possible complex anatomy of the occlusal area. The projection radiograph is obtained by means of an X-ray generator and an intraoral receptor. The principle of radiography relies on the properties of X-rays to be absorbed and scattered by hard tissues, such as dental tissues and bones, and to pass through soft tissues, such as skin and gengiva, reaching the receptor. Therefore, soft tissues appear dark on the film (or sensor in case of digital radiography), creating a radiopacity, while hard tissues, which absorb X-rays, appear brighter, creating a so-called radiolucency.

Different configurations are possible, such as panoramic, bitewing or pe-

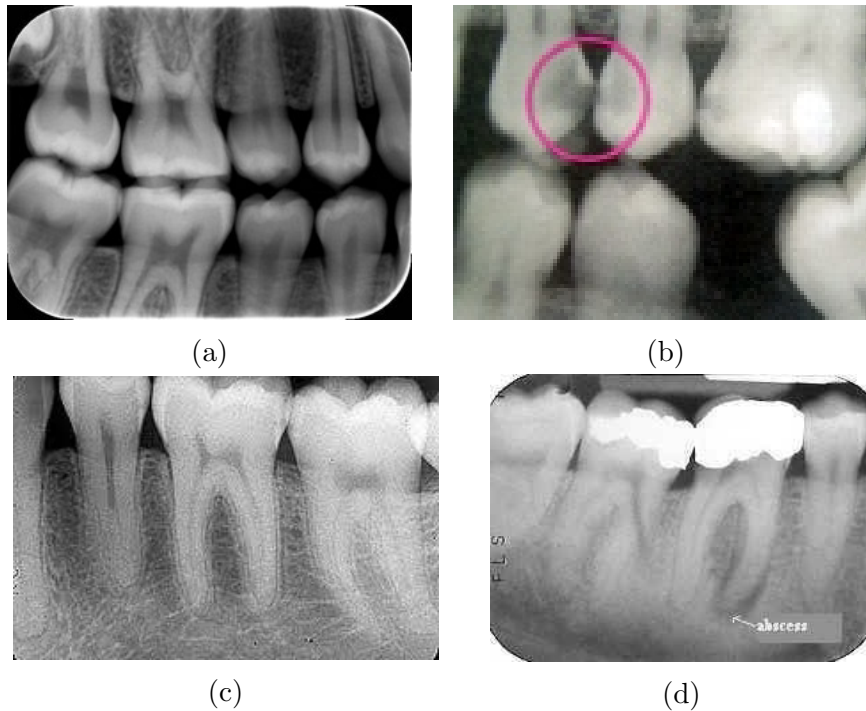


Figure 2.3: Configurations of dental intraoral radiography for caries detection: (a) Example of bitewing radiograph, (b) example of approximal lesion (circled) detected on a bitewing radiograph. Demineralised tissue is porous and this reduces the radiation absorption, creating radiolucency. (c) Example of periapical radiograph and (d) example of abscess (indicated by the arrow) detected on a periapical radiograph. In (d) fillings are clearly visible as they do not allow the radiation to pass through the tissue, absorb the photons, creating a radiopacity.

riapical. Bitewing radiographs (Figure 2.3a) are used for caries detection, especially suitable for approximal lesions (Figure 2.3b), and for caries screening, while periapical radiographs (Figure 2.3c) are used when the focus is on the single tooth. The scores used to evaluate radiographs are in Table 2.4. One of the main issues with radiography is that the scoring process is highly subjective[59]. While for approximal lesions bitewing radiographs can be considered a valid detection technique, even at early phases (scores 1 and 2) occlusal lesions are instead difficult to assess and the distinction among

Radiographical score	Definition
0	no radiolucency
1	radiolucency in outer half of the enamel
2	radiolucency in inner half of the enamel \pm EDJ
3	radiolucency limited to the outer third of dentine
4	radiolucency reaching the middle third of dentine
5	radiolucency reaching the inner third of dentine, clinically cavitated
6	radiolucency into the pulp, clinically cavitated

Table 2.4: Radiography: classification of lesion severity.

scores from 0 to 2 is impractical. This happens since radiography depends on several parameters, such as the level of porosity of the tissue, the depth of the lesion, the anatomy of the tooth, the natural thickness of the enamel, which is different for each tooth and for each mouth. For example, if the observed demineralisation is rarefied even though rather deep and spread, the resulting radiolucency may not be so obvious. This affects the radiography detection ability, which is both limited to severe cases, when operative treatments may already be necessary, and examiner dependent, where skill and experience of the observer are relevant. Moreover, radiography is affected by intra-observer variability and not only by a high inter-observer variability. This means that the same observer may give different scores to the same radiograph at different times. Moreover, the occurrences of false positive diagnosis, when a lesion is wrongly detected, and false negative diagnosis, when a lesion is present but not detected, greatly affect the performance of this method and this is why it is considered rather a decision-making support only for dentine lesion detection and screening. A compromise between diagnosis demand and radiograph frequency needs consideration. Due to the possible malignant effect of radiation on human tissue[60], new digital detectors have been designed with particular attention to radiation reduction. However, refining exposure time remains the most important aspect towards optimised patient doses. Therefore, it might be desirable to reduce the need for ra-

diographs, at least regarding their application on the detection of caries, for which they are still routinely required, and use them for providing dentists with information concerning bone health, tooth-bone structures and other pathologies difficult to assess otherwise.

Another possible application of radiography is lesion monitoring. With digital radiographs it is possible to compare serial radiographs taken with identical positioning and exposure settings. Digital subtraction radiography[8, 61] allows for qualitative assessment of caries progression or even quantitative periodontal bone loss. Although promising, the required repositioning precision is limiting this technique to research.

Another major limitation of intraoral radiography is the possibility of anatomical structures overlapping, due to the returned image, a two-dimensional buccal-lingual projection. This is a big issue when assessing approximal caries on overlapping crown surfaces for example (Figure 2.4). But projection er-

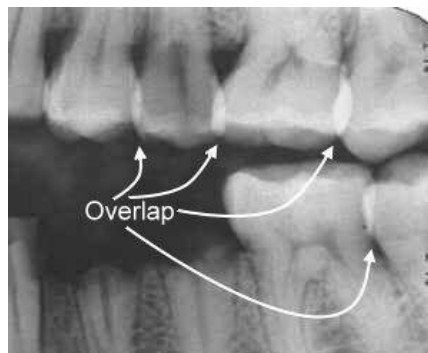


Figure 2.4: Example of overlap on a bitewing radiograph, obscuring any caries that may be present. Cases of overlap can occur either due to the anatomy of the examined mouth or to the misangulation of the X-ray beam, which should be perpendicular to the receptor.

rors may also lead to misinterpretation of the actual bone anatomy while assessing bone pathologies.

Although radiography has rapidly evolved in the last years with the use of X-rays for Computed Tomography, three-dimensional imaging is not suitable for application to dentistry, because it suffers from the same issue as in

the 2D version: this technique is prone to projection errors, which can create overlap of interproximal crown surfaces and prevent adequate caries diagnosis. Therefore, they are not recommended for diagnosis of caries lesions and panoramic or bitewing radiographs are still preferable.

2.6 Electronic Caries Monitor

Electronic Caries Monitor (ECM) is an instrument for caries detection based on measurement of electrical conductivity for evaluation of dental porosity. Porosity allows for penetration of fluid from the oral cavity into the tooth structure. Fluid contains ions that increase porous tooth electrical conductivity, or decrease electrical resistance or impedance[22].

The ECM device uses a single fixed-frequency alternating current and is



Figure 2.5: Electrical Caries Monitor: (a) site-specific and (b) surface-specific measurement modes.

provided with a probe with a co-axial airflow in order to dry the tissue around the probe and prevent current leakage. It has been assessed as having a good reproducibility[8, 62] but with non-random measurement variations showing clustering at low and high end of the measurement range. This can be explained with an insufficient and unpredictable probe contact for site-specific measurements (Figure 2.5a). Apart from site-specific measurements, there is also a surface-specific measurement mode (Figure 2.5b), which, though,



(a)



(b)

Figure 2.6: (a) Example of mild fluorosis, oral health condition where hypomineralisation affects enamel due to excess intake of fluoride during the dental eruption. (b) Example of MIH: oral health condition where hypomineralisation of enamel appears symmetrically among incisors or among molars. The etiology of MIH is still unclear.

produces different values and showed a lower efficacy causing the research community to focus on site-specific measurement studies.

A limitation of ECM is in the interpretation of the ECM returned value in relation with porosity. It is, in fact, not clear if the ECM result characterises the volume of the pores, pore depth or if it depends somehow on the morphological complexity of the pores. Moreover porosity does not vary because of caries only. It depends on maturation, a time-dependent decrease in porosity has been observed in newly erupted teeth, which are, then, more sensitive to caries attacks than normal teeth at the beginning[63]. Conditions such as fluorosis (Figure 2.6a) and hypomineralisation (molar incisor hypomineralisation, MIH) (Figure 2.6b) do affect porosity and ECM showed statistical relevant output variations when assessing these cases. Moreover, physical factors that affect ECM results are: the temperature of the tooth,

the thickness of the tissue[64], probe contact and within-tooth site differences.

For completeness, ECM values and interpretation are reported in Table 2.5. Note that the same returned value range can be associated to more than one clinical output, meaning that this differences may need to be resolved by other means, the most common being visual inspection, highly affected by subjectivity, as explained in section 2.2.

Table 2.5: ECM: classification of lesion severity (only occlusal).

ECM score	ECM value interval/Definition
0	[-0.45, 1.0]
1	[1.1, 3.0]
2	[3.1, 9.0]
3	[9.1, 12.0] Clinically ± microcavitated
4	[9.1, 12.0] Clinically shadowed
5	>12 Clinically cavitated but less than half of the surface
6	>12 Clinically cavitated but more than half of the surface

2.7 Near Infrared Transillumination and OCT

Near Infrared Transillumination (NIR-TI) imaging method is a technique for caries detection based on the transillumination of near infrared light typically at 1300 nm irradiating the cemento-enamel junction perpendicular to the buccal and lingual surfaces.

The limitations that visible light showed on caries detection encouraged studies on the properties of the interactions between near infrared light and dental tissue. At visible wavelength the main limit is sound enamel light scattering, obscuring access to information coming from the layers below, the enamel thickness and the dentine. Since it was known that dental tissue scattering coefficient decreased with increasing wavelength, sound enamel attenuation coefficients measured at 1310 nm and 1550 nm were studied, and

it was found that they are 1-2 orders of magnitude less than those in the visible range. This allowed for calculating the mean free path of photons in enamel, resulting in ~ 3 mm for 1310 nm and 1550 nm while it is about 0.1 mm for wavelengths in the visible range, namely 543 nm and 632 nm[28, 29]. At the beginning this technique was used to investigate interproximal enamel lesions only, but then the discovered high transparency of the enamel allowed for application to the visualisation of occlusal lesions as well[65](Figure 2.7). The theory behind the ability to detect deep lesions is related to the property of the dentine of being highly scattering. The dentine would scatter the light entering right under the enamel layer; then, since at 1300 nm, wavelength that showed the lowest attenuation coefficient, enamel was found to be almost transparent, attenuations of the diffused light would be mainly due to lesions in dentine (Figure 2.8).

It was also stated that measurements were not affected by fluorosis and

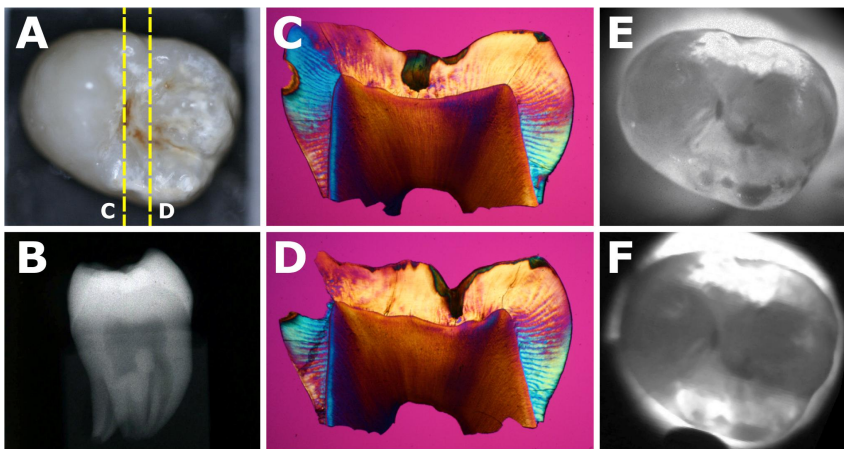


Figure 2.7: Example of NIR transillumination image of an enamel occlusal demineralisation. (A) Visible-light reflectance image, (B) radiograph, (C, D) polarized light microscopy images of the sections cut along the yellow dotted lines in (A). NIR transillumination images captured with the (E) Ge enhanced CMOS camera and (F) NIR imaging camera with the InGaAs focal plane array[66].

hypomineralisation, but the only proof was a visual evaluation of one image,

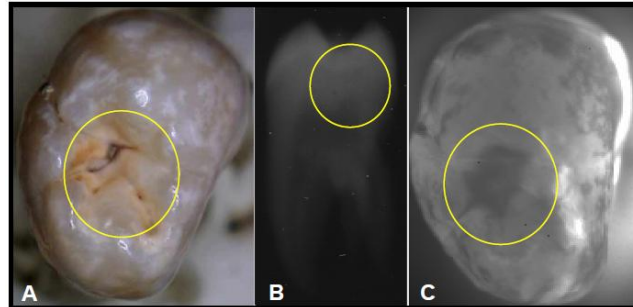


Figure 2.8: Example of NIR transillumination image of a dentine occlusal demineralisation. (A) Reflected white light image of molar with a large lesion (yellow circle) in the central fissure, (B) Radiograph, (C) NIR transillumination image[65].

not resulting in a clear evidence. Another study was more cautious about this topic, stating that it seemed that fluorosis appeared differently comparing to early caries on NIR images but that it is not possible to definitively distinguish them with certainty[67]. Further study is required on these aspects.

From a comparison between NIR transillumination and NIR reflectance, the latter being the main focus of this thesis, both at 1300 nm, it was found that NIR reflectance gave a better contrast than transillumination when detecting enamel demineralisations, while transillumination was better at determining dentine caries, although the difference in contrast between lesions confined to the first third of dentine and those confined to enamel was not statistically significant ($p > 0.05$). A near infrared multi-modal imaging method was then suggested. Other techniques were combined with NIR-TI with good results, namely with Optical Coherence Tomography (OCT) and Polarisation Sensitive OCT (PS-OCT)[68, 69, 70].

OCT was used on biological hard tissue in 1998 for the first time. The ability of imaging a cross-section of a whole tooth non-invasively, non-destructively measuring backscattered light intensity using long wavelengths, such as 1300 nm, opened a new field of research[31]. The principle of deminer-

alisation imaging with PS-OCT relies on the weak scattering generated by sound enamel in the near infrared, while the porosity present where demineralisation exists is a strong scatterer. Therefore, sound enamel produces a weak signal, which is further attenuated by scattering as the light penetrates in depth through the tooth. If demineralised enamel or dentine are present, they can be differentiated at optical depths of 2-3 mm (Figure 2.9).

NIR transillumination and PS-OCT were combined in an experiment of

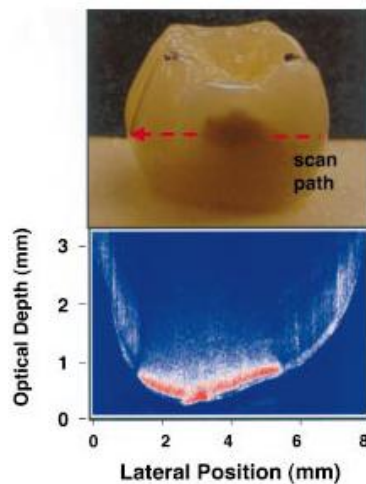


Figure 2.9: Example of PS-OCT image of a proximal demineralisation[68].

image-guided laser ablation[69]. NIR and PS-OCT images were compared in an exercise of detection of artificially created lesions and then NIR images were used as lesion maps to guide the action of a laser to ablate the caries lesions. Post-ablation images demonstrated the result of the treatment.

Some of the limitations of NIR transillumination are intrinsic of the illumination mode, as it was for FOTI. The light probe position may determine the success of the detection method; the non-uniformity of the transilluminated light striking one side of the tooth may result in variations of appearance depending on the relative orientation of the lesion and the source, also due to the varying amount of tissue the light must then travel. For example this

may create dark areas that may be confounded as demineralised areas or, viceversa, not clear illumination may cause a false negative score, missing an actual lesion.

Caries scores for this method are evaluated based on image contrast values. Contrast is calculated based on the line profile generated after the drawing by a trained user of lines passing on the lesion area and including sound tissues. The final values are then dependent on the user input, the availability of sound tissue around the investigated lesion, the direction of the incident light, the distance of the area of interest to the light source. For example, when the lesion is closer to the light source, lesions appear high in contrast; lesions further from the source are barely visible due to the high level of scattering that has occurred before reaching the lesion.

A very important consideration emerging from these studies was that near infrared light is not affected by stain.

Chapter 3

Histological validation of NIR reflectance multispectral imaging technique for caries detection and quantification

3.1 Introduction

Near infrared (NIR) multispectral imaging is a novel noninvasive technique that maps and quantifies dental caries. The technique has the ability to reduce the confounding effect of stain present on teeth. The aim of this study was to develop and validate a quantitative NIR multispectral imaging system for caries detection and assessment against a histological reference standard. The proposed technique is based on spectral imaging at specific wavelengths in the range from 1000 to 1700 nm. A total of 112 extracted teeth (molars and premolars) were used and images of occlusal surfaces at different wavelengths were acquired. Three spectral reflectance images were combined to generate a quantitative lesion map of the tooth. The maximum value of the map at the corresponding histological section was used as the

NIR caries score. The NIR caries score significantly correlated with the histological reference standard (Spearman's coefficient = 0.774, $p < 0.01$). Caries detection sensitivities and specificities of 72% and 91% for sound areas, 36% and 79% for lesions on the enamel and 82% and 69% for lesions in dentin were found. These results suggest that NIR spectral imaging is a novel and promising method for the detection, quantification and mapping of dental caries.

3.2 Description of the technique

Near infrared reflectance technique is an imaging method recently invented and developed with the aim of detecting occlusal caries lesions with a big advantage on most of the other methods: it is not affected by stain, the main confounding factor for visual inspection methods and those using light or fluorescence in the visible spectrum. Moreover, it aimed to return a map of lesions instead of a single-value diagnosis, giving also quantification of lesion severity. The principle relies on a near infrared hyperspectral study of den-

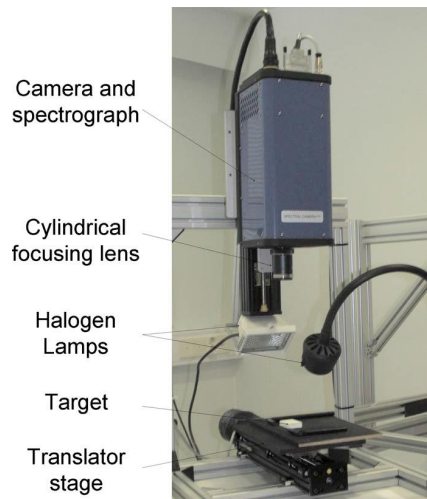


Figure 3.1: NIR hyperspectral imaging system.

tal samples carried out by Zakian et al.[9]. A picture of the hyperspectral imaging system is shown in Figure 3.1. The study consisted of measuring reflectance response of a pool of 12 teeth at wavelengths ranging between 1000 and 2500 nm, as shown in Figure 3.2, and the intuition that one wavelength response might be enough to discriminate between sound and demineralised tissues but it was not enough to discriminate enamel lesions from dentine lesions. Then, wavelengths were selected as containing the information required to give a caries score. The selected wavelengths had to reflect the information that porous enamel scatters more than sound enamel; dentinal caries contains fluid and the more severe the dentinal caries the more liquid it contains. Moreover, another wavelength was required as normalisation factor in order to adjust caries scores on a common scale and, therefore, make them comparable.

Six wavelengths were selected and the respective near infrared images

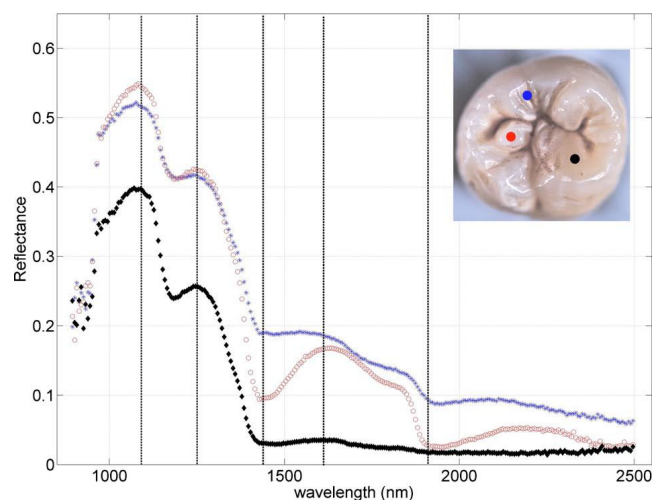


Figure 3.2: Example of reflectance response curves from 1000 to 2500 nm of an occlusal tooth surface for sound (black \blacklozenge), enamel lesion (blue $*$), and dentin lesion (red \circ) regions. The inset picture shows the location of the points selected within the tooth. Vertical dotted lines indicate the wavelengths chosen[9].

were investigated. NIR images of a tooth at the different wavelengths are

presented in Figure 3.3. The point of maximum on each region curve, at

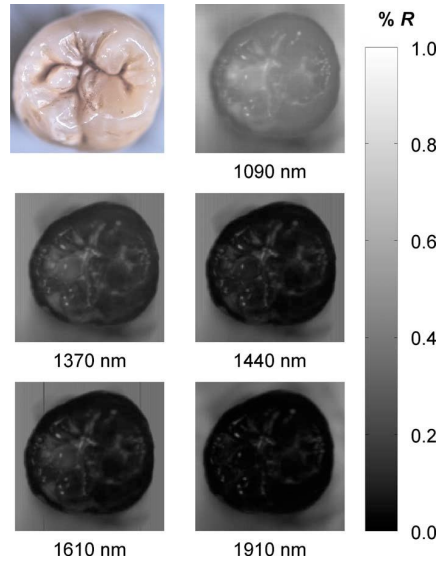


Figure 3.3: NIR hyperspectral imaging: selection of spectral images[9].

1090 nm, was selected to normalise the images in order to account for natural brightness and colour of the teeth. Reflectance values at 1370 nm showed a very clear distinction between sound and demineralised tissue. The wavelength of 1440 nm is the lowest wavelength where values corresponding to enamel demineralisations can be discriminated from dentine demineralisations and 1610 nm is the highest wavelength in the range under investigation where sound areas can be discriminated from lesion areas. It is known that the higher the wavelength the lower the scattering by sound enamel but also that at longer wavenlengths peaks of water absorption exist. Therefore, since the curve profile generated from sound tissues tends to zero as the wavelength increases as shown in Figure 3.2, scattering from enamel lesions and absorption from water in dentinal lesions should become more evident. In Figure 3.4 these phenomena are depicted. At 1440 nm there is also a peak of water absorption, so demineralised dentinal tissues register a lower reflectance value than enamel lesions, since the former are expected to have a larger fluid

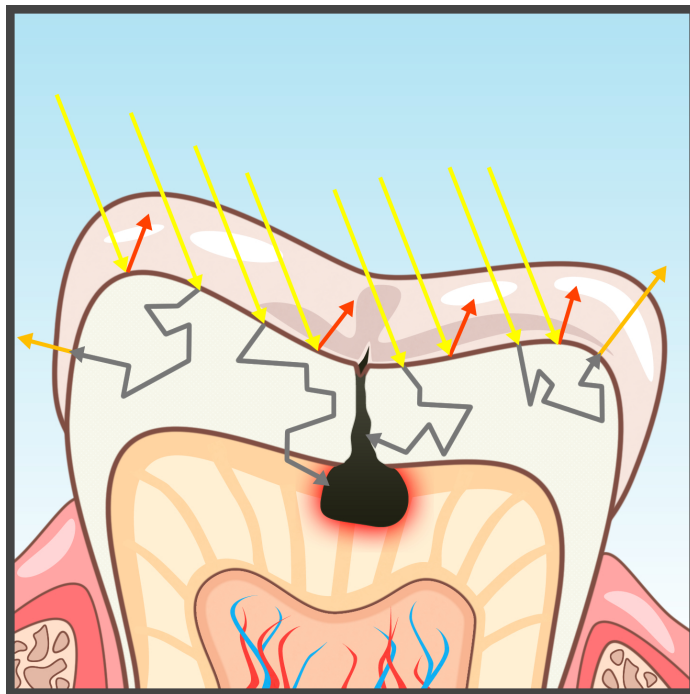


Figure 3.4: Illustration of a tooth section affected by dentinal caries and illuminated by NIR light (yellow arrows representing incident light). The events shown here are: specular reflections (red arrows), light scattering (gray/orange arrows) and water absorption by tissue severely affected by caries acting as a liquid *reservoir*. Note that this event may occur also in enamel if water is present. (Courtesy of Dr. Enrico Garavaglia)

content than the latter.

It was observed that these two wavelengths, 1440 and 1610 nm, together with the normalisation wavelength, 1090 nm, could be used for generating a caries score, using the formulas:

$$S_e = \frac{R(1610nm)}{R(1090nm)}, \quad (3.1)$$

$$S_d = \frac{R(1610nm) - R(1440nm)}{R(1090nm)}. \quad (3.2)$$

Then, a caries score S_{caries} was calculated as a combination of S_e and S_d :

$$S_{caries} = p \left(\frac{S_e - K_e}{N_e} \right) + (1 - p) \left(1 + \frac{S_d - K_d}{N_d} \right). \quad (3.3)$$

where e and d are for enamel and dentine, and K_e , K_d , N_e and N_d are calibration offset and normalisation factor, respectively. More details are in Zakian et al.[9]. Note that these factors are calculated empirically.

Examples of colour image, histological section and NIR S_{caries} image of teeth are shown in Figure 3.5. As it is possible to note on Figures 3.3 and 3.5, by the edges and crests of the teeth these images are affected by specular reflections. Since S_{caries} proportionally depends on the measure of reflectance, peaks of reflectance due to specular reflections become noise for the calculation of the score.

3.3 Materials and Methods

3.3.1 Sample Preparation

A set of 112 extracted teeth (premolars and molars) with natural lesions was collected from the Oral Health Centre of the University of Indiana, USA. Soft tissues were removed and thoroughly cleaned at this facility. Each tooth was immediately placed in a solution of distilled water and 0.1% thymol

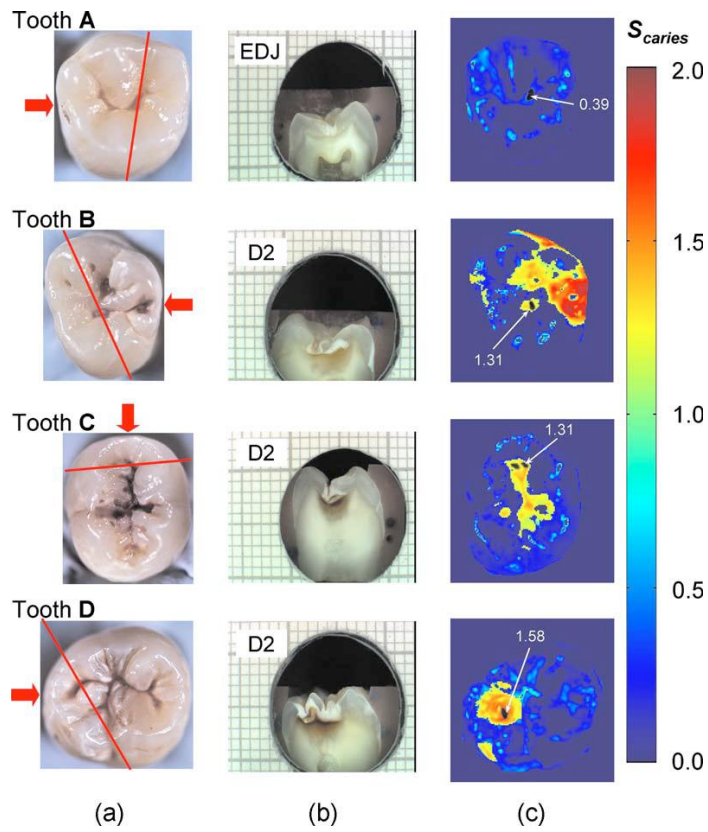


Figure 3.5: Examples of teeth with different carious lesions. (a) Colour picture for each tooth, (b) histological section indicated by the red line in the colour picture with the red arrow indicating the point of view of the section, (c) false-colour NIR caries maps, spatially scored using S_{caries} [9].

to prevent bacterial growth. Teeth were selected according to their ICDAS score ranging from 0 to 4 with the objective of having all lesion severities from none to the dentin across the sample set, but scores were not included in the analysis.

3.3.2 Instrumentation

A picture and a diagram of the NIR imaging setup are shown in Figures 3.6a and 3.6b. A near infrared multispectral imaging system was built

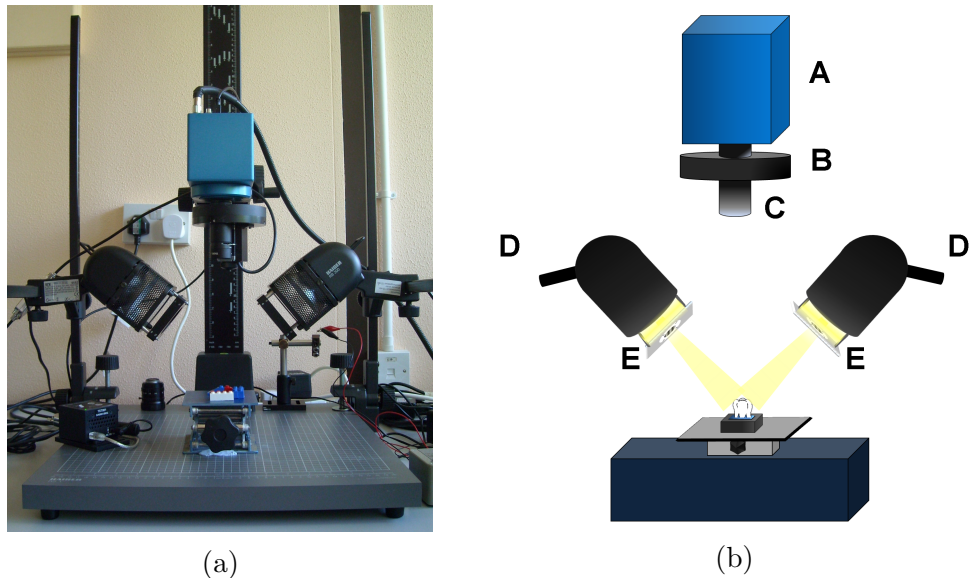


Figure 3.6: NIR multispectral imaging setup: (a) picture; (b) schematic diagram with InGaAs camera (A), filter wheel (B), NIR coated lens and polariser (C), halogen lamps (D) and polarisers (E). These polarisers were mounted orthogonally to the polariser in (C).

using an InGaAs camera (XEVA-FPA-1.7, XenICs), with a spectral response range from 0.9 to 1.7 μm , connected to a computer-controlled filter wheel with six filter positions. An extension tube with a NIR polariser (Thorlabs NIR Linear Polariser, 650 to 2000 nm) was mounted in front of the filter wheel. A 60 mm focal length NIR coated lens (Thorlabs AC254-060-C-ML)

was used to focus the sample image and an iris was attached in the front in order to increase the depth of field and reduce aberrations. Following the knowledge from a previous study[9], as described in section 3.2, the filter wheel was fitted with filters in the range from 1050 to 1600 nm, namely 1050, 1250, 1300, 1450, 1550 and 1600 nm, now taking also into account market availability of light sources for future works. Two broadband halogen lamps emitting visible and NIR light up to $2.5 \mu\text{m}$ (Osram 300W Halogen lamps) at about 30 deg from the horizontal plane were used for the illumination system and polarisers were mounted in front of each lamp, both cross-polarised with respect to the camera polariser. This removed specular reflections coming from the surface of the sample. A software application was developed for automatic image capture and filter selection.

3.3.3 Measurement Methodology

Each tooth was kept in the 0.1% thymol solution at room temperature before imaging. The samples were taken out of the bottle and placed on the sample holder only during measurement to prevent dehydration. Each tooth was placed with its occlusal surface facing the camera at a distance of 15 cm from the lens and air-dried for 15 seconds at approximately 5 cm to remove moisture from the enamel surface.

3.3.4 Histology

Tooth histology was used as the caries reference standard. Histology is the most common gold standard[24, 9, 71, 72, 73] and accepted as the most suitable for complete process validations and occlusal caries lesions[74]. It has a direct clinical relevance as it takes into account both physiological and structural changes related to the carious disease.

A relevant occlusal area with a suspected lesion was selected based on the ICDAS criteria[17] by two dentists (J.G./R.E.) and used as a region of

interest (ROI) on each tooth. In order to assess lesion severity at the specific point of interest, the individual teeth were mounted in acrylic resin blocks and hemi-sectioned in the bucco-lingual direction through the ROI using a 300- μm -thick diamond wheel saw (South Bay Technology inc., USA). Colour photographs of the hemi-sections were captured with constant illumination and magnification, as shown in Figure 3.7.

The images of the two hemi-sections obtained for each tooth were scored

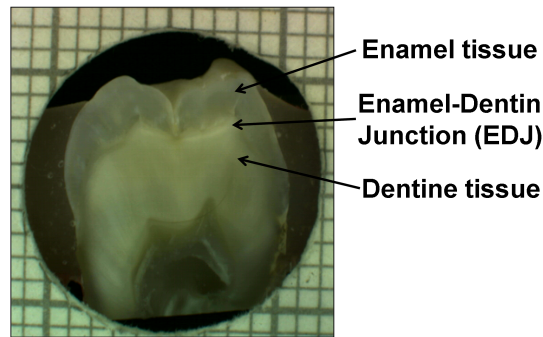


Figure 3.7: Example of a histological hemi-section.

by two examiners (J.G./I.P.) until agreement was reached and the final score was based on the highest score identified for the ROIs. The score criteria used were S for sound, E1 for a lesion up to the outer half of the enamel, E2 for a lesion to the inner half of the enamel, EDJ for a lesion up to the enamel-dentin junction, D for a lesion in dentin[9, 75].

3.3.5 Image Analysis

Images were pre-processed in order to obtain denoised and calibrated spectral reflectance images. Four reflectance standards at 2, 10, 50, 99% (Avian Technologies Gray Scale Standards) were captured for each wavelength at the beginning of the study to linearise the camera intensity to reflectance values. Illumination intensity variations were corrected by capturing an image of the 50% reflectance standard before each measurement and compensating for

the difference to a baseline reference value. A non-linear Gaussian filter was applied to denoise the image. The heterogeneity of the illumination spatial distribution was corrected by calculating a spatial distribution factor based on the image obtained from the 50% reflectance standard. The resulting calibrated images are shown in Figure 3.8 at the six wavelengths.

Based on the study described in section 3.2, calibrated reflectance spec-

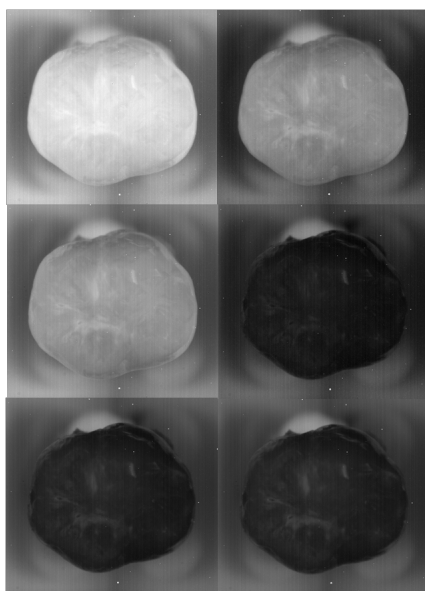


Figure 3.8: Example of calibrated NIR polarised images at six investigated wavelengths, 1050, 1250, 1300, 1450, 1550, 1600 nm.

tral images, R_λ , at $\lambda=1050$ nm, $\lambda=1450$ nm and $\lambda=1600$ nm were combined to generate a first functional image to detect the existence of a carious lesion, S_e , and a second functional image to quantify the severity of the detected caries lesion, S_d . They were calculated as follows:

$$S_e(i, j) = \frac{R_{1600}(i, j)}{R_{1050}(i, j)} \quad (3.4)$$

$$S_d(i, j) = \frac{R_{1600}(i, j) - R_{1450}(i, j)}{R_{1050}(i, j)} \quad (3.5)$$

where i and j are the coordinates of each pixel of the images. In the above equations, R_{1600} provides information on the light scattered by the surface (which would be related to enamel lesions), while R_{1450} provides information on both the light scattered by the surface (due to enamel lesions) and the attenuation of light due to water absorption (which would be related to dentin lesions). Note that the natural brightness of each sample is also accounted by normalising the images by R_{1050} . Figure 3.9 shows example images for S_e and S_d . A caries map, S_{caries} , was then obtained by identifying presence or

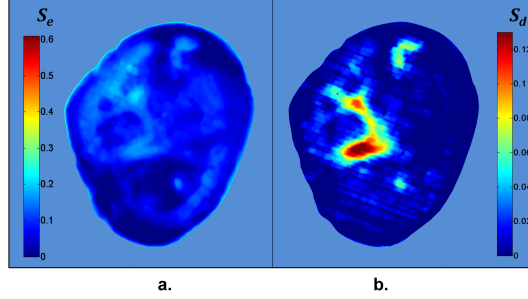


Figure 3.9: Examples of NIR images for S_e (a) and S_d (b). S_e gives information on presence and position of lesions while S_d quantifies the severity of the lesions giving a continuous score pixel by pixel.

absence of caries using S_e and quantifying it using S_d , combined as follows:

$$S_{caries}(i, j) = \begin{cases} 0 & \text{if } S_e < th_e \\ S_d(i, j) & \text{otherwise} \end{cases} \quad (3.6)$$

where th_e is the threshold for S_e to detect presence of lesions. The precise threshold value is found following the statistical analysis described in the next section.

Although the selection of wavelengths and Equations 3.1 and 3.2 are based on a previous publication [9], the need of empirical factors for S_{caries} is eliminated in here by calculating the thresholds based on the statistical analysis described below.

3.3.6 Statistical Analysis

A region of interest was selected for each caries map corresponding to the site of the most representative histological hemi-section. The maximum S_{caries} value inside the region was used as the S_{caries} score for the tooth. Teeth were sorted by histological score with the odd and even entries split into two sub-sets: training sample set (56 teeth) and test sample set (56 teeth). This allowed for an equal lesion severity distribution across both sets.

Receiver Operating Characteristic (ROC) analysis was performed to determine the diagnostic accuracy of the method. ROC curves are created by plotting the fraction of true positives out of the positives (sensitivity) versus the fraction of false positives out of the negatives (1-specificity, where specificity is the fraction of true negatives out of those scored as negative), at various threshold settings. ROC analysis was then used to select the optimal thresholds, which maximise (sensitivity, specificity) couples, and to discard suboptimal ones.

ROC curves were calculated on the training sample set to find detection thresholds corresponding to the best Youden's index (sensitivity + specificity - 1) for each histology level, namely E1, E2, EDJ and D; an ideal index value would be one. Note that using this same methodology, th_e was calculated from S_e at the E1 histology detection level and subsequently used to generate S_{caries} maps as described in Equation 3.6.

A three level detection analysis was implemented with these thresholds in order to investigate the ability of the NIR imaging system to classify (a) areas with no lesion ($S_{caries} = 0$), (b) areas with enamel lesion ($0 < S_{caries} < th_d$) and (c) areas with dentine lesion ($S_{caries} \geq th_d$). Here th_d corresponds to the threshold value for the detection of lesions at the D histology level as calculated from S_{caries} . Areas with enamel lesion include cases with demineralization in the outer half of the enamel (E1), inner half of the enamel (E2) and at the enamel-dentine junction (EDJ). A confidence table was computed for the three-level classification to calculate the sensitivity and specificity of

NIR against histological reference standard.

The S_{caries} threshold optimised for the training sample set was then applied to the test sample set to produce an unbiased classification analysis and evaluate the ability of the method proposed on an independent (test) set of data.

Spearman's correlation was used to investigate the relationship between the histological and the S_{caries} scores.

3.4 Results

Examples of near-infrared maps are shown in Figure 3.10. A line on the related colour picture indicates the location where the tooth was sectioned, corresponding to the ROI where the S_{caries} score was obtained. The three cases in Figure 3.10 show increasing lesion severity in the histology sections, and this is reflected on the S_{caries} score as expected. The maps show a continuous scale above zero as severity increases. Values of zero on the S_{caries} map are therefore registered as sound; values above zero and below $th_d = 0.0718$ ($0 < S_{caries} < 0.0718$) are registered as enamel lesions, otherwise as dentine lesions. Figure 3.11 shows boxplots of S_{caries} and histological scores for the training and the test sets.

The mean and the standard deviation of the S_{caries} values for each histological score are presented in Table 3.1. In Table 3.2, confidence tables for these two sets are also shown.

Table 3.3 presents the threshold values for S_{caries} and S_d calculated using the ROC curve analysis from the training sample set. Note that the areas under the ROC curve for the training sample set give a measure of detection accuracy (with ideal value of 1), ranging from 0.90 to 0.94 for S_{caries} . The corresponding sensitivity and specificities for each set is also shown along with the Youden's indices both for training and for test sets. The best Youden's index for S_{caries} is 0.93 obtained at the E1 level, discrim-

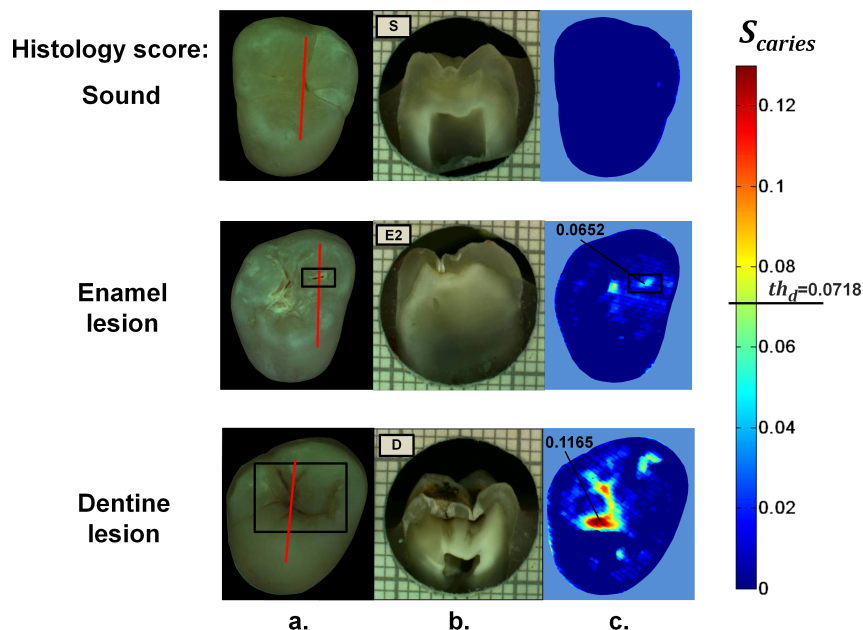


Figure 3.10: Examples of NIR images for S_{caries} . Three different cases: sound (top), enamel lesion (middle) and dentine lesion (bottom). For each tooth the colour picture (a) with the indication of the investigated lesion (black square) and the histological sectioning site (red line), the corresponding histological section (b) and the false-colour S_{caries} map (c) are shown. On the colour bar the range of S_{caries} values are shown along with the dentine lesion threshold ($t_{hd} = 0.0718$). Values of zero on the S_{caries} map are registered as sound; values above zero and below thd ($0 < S_{caries} < 0.0718$) are registered as enamel lesions, otherwise as dentine lesions.

Table 3.1: Table of mean and standard deviation values for training sample set and test sample set.

<i>Training set</i>				<i>Test set</i>			
Histology	Mean	N	Std. deviation	Histology	Mean	N	Std. deviation
Sound	0.0067342	12	0.01664017	Sound	0.0103640	11	0.02333643
E1	0.0337573	2	0.04774006	E1	0.0247635	2	0.03502086
E2	0.0617351	8	0.02722018	E2	0.0630870	9	0.02652615
EDJ	0.0650418	11	0.03049387	EDJ	0.0696345	11	0.02790564
Dentine	0.0952079	23	0.02419613	Dentine	0.0982882	23	0.02846444

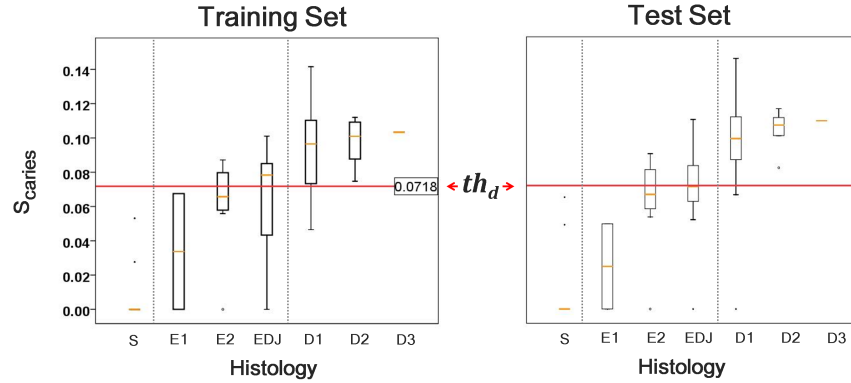


Figure 3.11: Boxplots of $S_{carries}$ against histological scores. $S_{carries}$ scores from training set on the left and from test set on the right. The red horizontal lines represent the $S_{carries}$ threshold (th_d) at the D histology level, calculated based on the training sample set and applied to the test sample set. The D histology level is here decomposed in its components: D1 (first third of dentine), D2 (second third of dentine) and D3 (last third of dentine).

Table 3.2: Confidence table for training sample set (a) and test sample set (b).

		<i>NIR spectral imaging</i>		
		Sound	E1 + E2 +EDJ	Dentine
(a) Training set				
Histology	Sound	12	0	0
	E1 + E2 +EDJ	2	12	7
	Dentine	1	0	22
		<i>NIR spectral imaging</i>		
		Sound	E1 + E2 +EDJ	Dentine
(b) Test set				
Histology	Sound	8	3	0
	E1 + E2 +EDJ	4	8	10
	Dentine	0	4	19

Table 3.3: Values of thresholds, areas under the curve, sensitivities, specificities, and Youden's indices at each lesion level (for histology score greater or equal to E1, E2, EDJ, or D) are shown for S_{caries} and S_d . Results are divided in training sample set (half of the sample population on which thresholds were calculated) and test sample set (remaining half of sample population on which thresholds were applied).

	S_{caries} training set					S_{caries} test set		
	Threshold	Area	Sensitivity	Specificity	Youden's	Sens.ty	Sp.ty	Youden's
$h \geq E1$	0.0277	0.93	93%	>99%	0.93	91%	73%	0.64
$h \geq E2$	0.0278	0.94	95%	93%	0.88	93%	69%	0.62
$h \geq EDJ$	0.0676	0.91	88%	86%	0.75	74%	82%	0.56
$h \geq D$	0.0718	0.90	96%	79%	0.74	83%	70%	0.53
	S_d training set					S_d test set		
	Threshold	Area	Sensitivity	Specificity	Youden's	Sens.ty	Sp.ty	Youden's
$h \geq E1$	0.0556	0.96	89%	>99%	0.89	91%	64%	0.55
$h \geq E2$	0.0557	0.96	90%	93%	0.83	95%	69%	0.64
$h \geq EDJ$	0.0676	0.91	88%	86%	0.75	79%	77%	0.56
$h \geq D$	0.0718	0.91	96%	76%	0.71	87%	67%	0.54

inating between sound tissue and lesion. Lesion detection sensitivities above 88% and specificities above 79% were found for S_{caries} .

For the test sample set the highest Youden's index found was 0.64 at the E1 level. S_{caries} shows high sensitivity (91%) and good specificity (73%) at detecting lesions at the outer half of the enamel (E1) and above. Moreover, severe demineralization (D) was detected with 83% sensitivity and 70% specificity.

Results for another possible NIR score, S_d , are shown. S_d is proposed as a simplification of the score system but equally efficient (values for the area under the ROC curve ranged from 0.91 to 0.96), less sensitive to sound sites but more sensitive at detecting dentinal lesions. This is because S_{caries} has a higher specificity at the E1 level and therefore higher sensitivity at identifying sound areas, which results from the performance of the enamel threshold, th_e for S_e , as described in Equation 3.6. Note in Table 3.3 a higher sensitivity (95%) and specificity (69%) for S_d at the E2 histological level and

Table 3.4: Values of sensitivities and specificities at three lesion levels (for histology scores equal to S, E1 + E2 + EDJ or D) are shown for S_{caries} and S_d . Results are divided in training and test sample sets, as for Table 3.3.

Training set	S_{caries}		S_d	
	Sensitivity (%)	Specificity (%)	Sensitivity (%)	Specificity(%)
Sound	> 99	93	> 99	89
E1 + E2 +EDJ	57	> 99	43	> 99
Dentine	96	79	96	76

Test set	S_{caries}		S_d	
	Sensitivity (%)	Specificity (%)	Sensitivity (%)	Specificity (%)
Sound	73	91	64	91
E1 + E2 +EDJ	36	79	36	82
Dentine	83	70	87	67

also at the dentine level (87% and 67%) for S_d .

In Table 3.4, values of sensitivity and specificity for S_{caries} and S_d are shown both for training and test sets divided in three detection levels: (a) sites with no lesions, (b) sites with lesions at the outer half of the enamel, reaching the inner half of the enamel or reaching the EDJ; and (c) areas with lesions in dentine. This table is computed by applying the thresholds for detection of lesions at E1 level ($S_{caries} > 0$) and at D level ($S_{caries} \geq 0.0718$).

S_{caries} had a sensitivity and specificity of 99% and 93% for sound tissue, 57% and 99% for enamel lesion and 96% and 79% for dentine lesion detection on the training sample set. On the test sample set, S_{caries} had a sensitivity and specificity of 73% and 91% for sound tissue, 36% and 79% for enamel lesion and 83% and 70% for dentine lesion detection. S_d performed very similarly, with a lower sensitivity at detecting sound sites but higher sensitivity for dentine lesions, as shown in Table 3.4.

Significant Spearman's correlation coefficients of 0.774 ($p < 0.01$) between S_{caries} and histological scores and of 0.765 ($p < 0.01$) between S_d and histological scores were obtained.

A study was also carried out about how specular reflections affect the

Table 3.5: Results of sensitivity and specificity of S_{caries} at three lesion levels, sound, enamel lesions and dentine lesions, for the unpolarised set-up experiment are compared with the results from the polarised experiment. Results are divided in training and test sample sets.

Training set	$S_{caries-unpol}$		$S_{caries-pol}$	
	Sensitivity (%)	Specificity (%)	Sensitivity (%)	Specificity(%)
Sound	> 99	45	> 99	93
E1 + E2 +EDJ	27	91	57	> 99
Dentine	50	> 99	96	79

Test set	$S_{caries-unpol}$		$S_{caries-pol}$	
	Sensitivity (%)	Specificity (%)	Sensitivity (%)	Specificity (%)
Sound	> 99	27	73	91
E1 + E2 +EDJ	5	94	36	79
Dentine	35	97	83	70

S_{caries} score. Images of 250 teeth were captured by the set-up shown in Figure 3.6, with and without polarisers. Although cross polarisation dramatically reduces the light intensity and, thus, the detected signal, it was evident that this kind of noise limited the intrinsic principle and worth of the NIR method. Specular reflections were a big confounding factor both for the lesion visualisation and for the NIR score system. They were responsible for such an increase of the reflectance value in the area of the crests and around the crests that it was often impossible to distinguish good signal by specular reflections. Depending on the anatomy of the tooth, the noise could significantly cover areas of lesions, as when the occlusal area is made of many little crests interleaving with the fissure lines.

After calibrating the images and calculating S_{caries} for all of them, as described in section 3.3.5, and after histological reference standard was performed, sensitivity and specificity were obtained for a sample set of 112 teeth, as described in section 3.3.6. Results are presented in Table 3.5 and can be compared with those obtained from the polarised experiment, presented in Table 3.4, reported here for ease of comparison. Sensitivity to disease, both

at the enamel and dentine levels, is radically affected by specular reflections. This means that polarisers mounted at the light sources and at the detector orthogonally each other actually solved the issue of the specular reflections.

The common most remarkable advantage on these studies was that stain did not interfere with measurements.

3.5 Discussion

The NIR reflectance multi-spectral imaging method detects the change in porosity of the surface (a proxy for measure for mineral loss within enamel[6]) and reveals the presence of cavities under the surface, thus producing a detailed map of caries of the occlusal view of the tooth. Superficial changes in porosity would result in an increase of light scattering, whereas larger cavities would act as water reservoirs. Moreover, at longer wavelengths the scattering from sound enamel reduces, gaining a deeper penetration in the tissue. Presence of water in the lesion can be detected by NIR light absorption resulting in reflectance attenuation, particularly at about 1450 nm. It is judged that the increase of light scattering at 1600 nm may be used to account for superficial changes in porosity and therefore the difference between the reflectance at 1600 nm and at 1450 nm could explain the discrimination observed between enamel mineral loss and dentinal lesion. The initial near-infrared hyper-spectral study carried by Zakian et al.[9] revealed the caries detection ability of different wavelengths in the NIR spectrum.

Although the results reported previously using NIR reflectance imaging were promising, the study employed a small sample set of 12 teeth. A sensitivity and a specificity of > 99% and 87.5% for enamel lesions and 80% and > 99% for dentine lesions were reported. Note that as there was no split between training and test sample sets, the equivalent sensitivity and specificity in this study would be that the one for E1 level (93% and > 99%, respectively) and the one for D level (96% and 79%, respectively) in the training

set in Table 3.3.

In this study, the image quality and detection ability are improved by adding a system of cross-polarization of light in order to remove specular reflections. These reflections from the tooth surface acted as noise, preventing the lesions from being detected in affected areas. Moreover, on the study reported by Zakian et al.[9], empirical factors including the threshold values were applied to the algorithm which prevented generalization of the model. A considerable increase in the sample population, from 12 to 112, allowed more powerful statistical analysis and robust assessment of the technology. In order to evaluate the use of this method throughout the different disease stages, a full range of lesion severity was included in this study: 23 teeth were sound, 43 had lesions in the E1 (4), E2 (17) or EDJ (22), and 46 had dentine lesions. The diagnostic dilemma is separating enamel from dentine lesions and hence it is important to identify lesions just into dentine (1/3 or so up to pulp) as lesions larger than this may trigger operative interventions. Similarly, failing to detect this kind of lesions may lead unnecessary procedures to be carried out. Optimum thresholds were obtained quantitatively based on the ROC curves using the training sample set and applied to the test sample set. The use of two different sample sets for calculating the performance allows for an unbiased analysis where the test sample set is independent from the training sample set and represents the more realistic scenario where caries quantification would be performed on cases never measured before. It has been therefore shown that S_{caries} can be free of empirical factors, meaning that these findings are directly applicable to any new sample set.

The three-level detection statistical method[75] used in here can further inform the dental clinicians for a better decision-making. Computed on the test sample set, the S_{caries} score system results are very specific (91%) at detecting sound sites, meaning that unhealthy sites are truly detected as unhealthy and has a good performance at detecting demineralised dentine tissue

(sensitivity of 83% and specificity of 70%). Although quite specific (79%) at detecting enamel demineralization sites, both incipient and progressed (E1 to EDJ), the sensitivity is low (36%). This can be partly due to the limited presence of early enamel lesion cases in the sample set, affecting the threshold decision procedure (ROC curves) and therefore reducing the ability to discriminate between sound and incipient demineralization. This is a common issue for *in vitro* studies since the collection of samples with incipient natural lesions would mainly result from extractions due to orthodontic reasons. However, the low sensitivity is mostly due to severe lesions in the EDJ that were detected as dentine lesions. An example is shown in Figure 3.12. Consequently, this decreases the value of specificity at detecting dentine. The

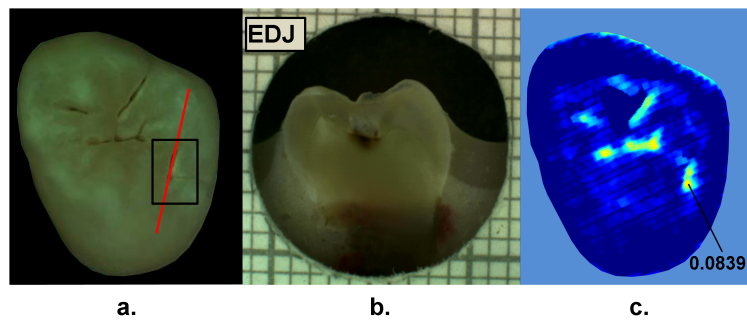


Figure 3.12: Example of overscoring. Colour picture (a); histological section (b); and S_{caries} map (c) of a tooth where S_{caries} scored above the dentine lesion threshold (0.0718).

probable cause of this issue is that the NIR method quantifies severity based on the presence of water. If a lesion is severe and very confined in the tissue at an EDJ level, it might contain more water than incipient lesions and S_{caries} would yield higher values.

Other cases of overscoring are presented. As shown in Figure 3.13, enamel breaks or enamel defects are detected as lesions even if scored as sound by histology. Note that the evaluation of the histological sections remains a subjective process but is however accepted as a gold standard. Scores are given on the basis of lesion depth and cannot give information on activity

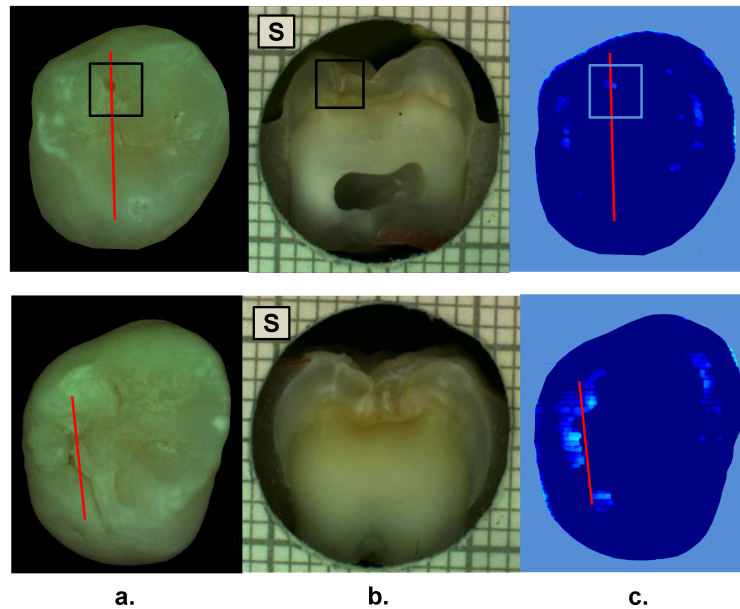


Figure 3.13: Examples of overscoring. Colour pictures (a); histological sections (b); and S_{caries} maps (c) are shown. Enamel break (top) and enamel defects (bottom) scored by histology as sound but detected as enamel lesion.

in the lesion or remineralization of the tissue (it is broadly based on colour changes in the tooth structure rather than assessment of infected or affected tissues). Although more studies on the NIR response on remineralised tissue are required, when the tissue is remineralised, a reduced porosity is expected and therefore lower scattered light could be detected and scored as sound. However, if there is enamel breakdown, this might be detected as lesion even if scored as sound with histology, as shown in the top image in Figure 3.13.

Very few cases of underscoring were reported, an example is shown in Figure 3.14. Underscoring can be due to an excess of moisture filling the porous tissue, reducing the amount of light scattering at 1600 nm and lowering the values for S_{caries} . Although Chung et al.[76] suggested that use of reflectance to determine lesion depth was inappropriate due to a reduced penetration of light in the presence of lesions, this would not explain the overall behaviour observed in our study. In fact, using the spectral difference

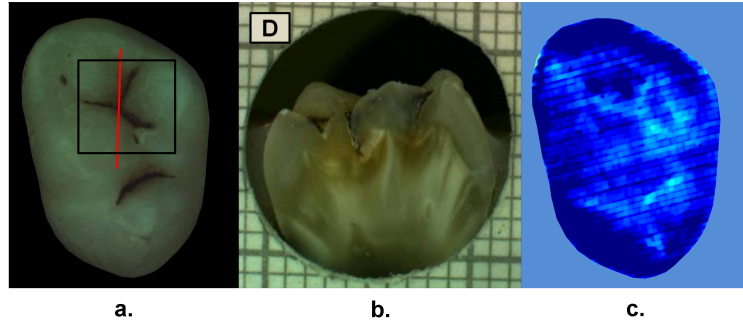


Figure 3.14: Example of underscoring. Colour picture (a); histological section (b); and $S_{carries}$ map (c) of a tooth with dentine lesions that was scored by $S_{carries}$ as demineralised up to the inner half of enamel. Possibly the presence of water in the enamel attenuated the reflectance at 1600 nm.

between R_{1600} and R_{1450} allows for a clear distinction between dentine lesions under overlying enamel lesions, as R_{1450} is affected by water even in presence of scattering due to surface porosity. Moreover, the relative combination of specific wavelengths for imaging reduces the influence of the natural tooth reflectance variations on the quantitative caries score. This approach allows for an automated distinction between sound tissue and demineralised tissue without requiring the input of a user to preselect specific regions of interest such as sound areas surrounding the lesion or sound edges at the extreme ends of a line profile drawn for quantification. This is aimed to reduce any source of subjective information introduced about the tooth in the method.

From the results obtained in this study, it was observed that higher severity corresponded to higher demineralization. In most cases this would coincide with increased depth, but this is not necessarily true, as in the examples shown in Figures 3.12 and 3.15.

Unlike single point measurement devices, the lesion mapping ability of the technique presented can be an instantaneous visual enhancement tool for the clinicians. Mapping the tooth using NIR light can help to discriminate between a stained healthy site and a site with stained-carious tissue. In Figure 3.16, two examples of stained teeth are shown. In the first case

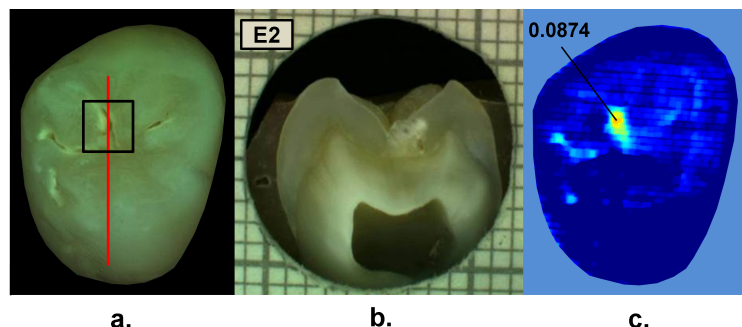


Figure 3.15: Example of overscoring. Colour picture (a); histological section (b); and $S_{carries}$ map (c) of a tooth with enamel lesion scored as dentine by $S_{carries}$ (dentine lesion threshold $th_d = 0.0718$).

(top images) the colour image shows a stained fissure pattern that covers the lesion as mapped by $S_{carries}$, while in the second case (bottom images) the stain pattern is invisible to the lesion pattern indicated by $S_{carries}$. This suggests that stain is neither increasing nor decreasing the $S_{carries}$ measurement. In both cases stain negligibly absorbs NIR light[9, 77] and $S_{carries}$ maps the lesions present at different levels demonstrating that the stain does not interfere with the NIR imaging. Stain is the biggest confounding factor in techniques using visible light such as QLF and DIAGNOdent, as well as clinical inspection and FOTI and DIFOTI. Moreover, NIR light is noninvasive and can be used as frequently as required. The restrictions of this technique may be the presence of large enamel breaks, such as macroscopic holes on the surface.

As already reported in Zakian et al.[9], this case is easily detectable with visible inspection to which this technique is suggested as an adjunct to support decision-making. It, however, performs efficiently in the case of microcavities, where microscopic holes on the enamel, difficult to detect, are channels to extended severe caries in dentine.

Detection improvements can be investigated by modifying the measurement procedure and the detection algorithm. This technique ideally requires dry enamel in order to detect the presence of water in dentine. Further stud-

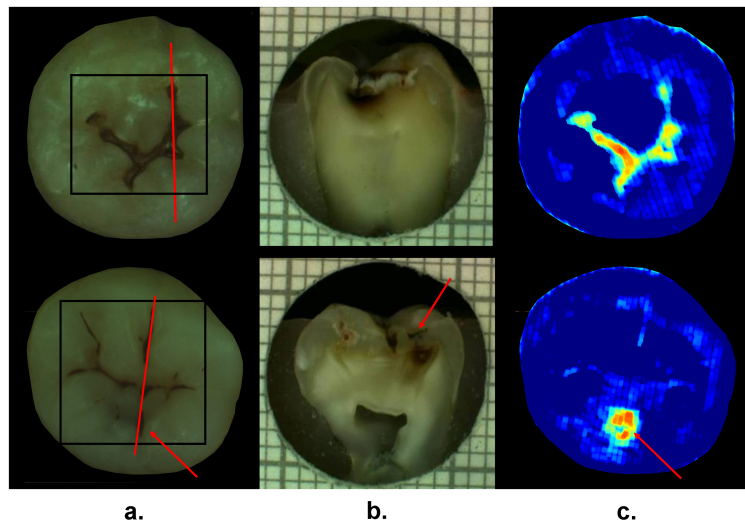


Figure 3.16: Examples of teeth affected by stain. Colour pictures (a); histological sections (b); and S_{caries} maps (c) are shown. These cases demonstrate the ability of S_{caries} to detect dental caries through stain. S_{caries} is able to map dentinal lesions underneath a layer of stained tissue as seen in the upper case. The tooth shown in the bottom is used to confirm that the map is not affected by stain as the stain pattern visible in the corresponding colour image is not reflected in the map. Arrows show how the stain does not interfere with the detection of the spread dentinal lesion underneath.

ies can be undertaken with a dynamic drying system computer-controlled for concurrent monitoring of the signal. The results are encouraging and other types of carious lesions could be assessed in future work, such as fluorosis and approximal lesions.

3.6 Conclusions

In this study, 112 teeth were examined with the NIR multispectral imaging and hemi-sectioned to validate this technique against a histological reference sample. NIR can detect sound tissue with sensitivity and specificity of 73% and 91%, enamel lesions with 36% and 79%, and dentine lesions with 83% and 70%.

This NIR technique is noninvasive, stain insensitive, and it has the ability of mapping the tooth showing the presence of lesions and giving a continuous caries score pixel by pixel. This technique can be a tool for detection of early to severe caries, can help the clinician in first assessment and dental health monitoring, can give information on the location of the lesion for targeted treatment procedures, and can enhance communication with patients, as recently recognised and suggested as an essential objective for dental practitioners[5].

Chapter 4

Comparison of NIR Reflectance Multispectral Imaging Technique with Conventional Caries Detection Methods

4.1 Introduction

Objectives: To compare the occlusal fissure caries detection ability of near-infrared reflectance(NIR) multispectral imaging to two clinical visual scoring techniques, namely International Caries Detection Assessment System (ICDAS) and Fibre-Optic Transillumination (FOTI), and to radiography and Quantitative Light-induced Fluorescence (QLF). These are among the main techniques currently used clinically and in research. **Methods:** Occlusal lesions of a sample set of 110 extracted teeth (premolars and molars) were examined with all the techniques and histology was used as the reference standard. Caries detection sensitivity and specificity were used to compare the techniques. **Results:** Visual inspection methods recorded the highest values of sensitivity (ICDAS: > 99%, FOTI: 93%) and specificity to dental

caries (FOTI: > 99%, ICDAS: 90%). However, these methods could have been highly facilitated by the in-vitro viewing of the samples. Sensitivity to dental caries was higher for NIR (91%) than for QLF (88%) and radiography (63%) while specificity was higher for radiography (81%) than for NIR (73%) and QLF (63%). **Conclusions:** The NIR method offers objective supporting information to quantify and detect dental caries and is especially suitable for areas affected by confounding factors such as stain, affecting ICDAS, FOTI and QLF. NIR and QLF both help visualising the lesions and provide an alternative view (occlusal) to radiography without ionising radiation. **Clinical significance:** the NIR method has the ability to detect dental caries when other methods fail, assist in the decision making process and aid monitoring of preventive interventions; it can enhance patient communication and in some cases avoid the use of radiographs.

4.2 Materials and Methods

4.2.1 Sample preparation

110 out of 257 extracted human teeth (premolars and molars) with natural occurring occlusal caries lesions were selected according to their ICDAS score with the intention of including samples with lesions of varied severities for the study. Note that histology could not be used at the selection stage as it is a destructive method. The teeth were collected from the Oral Health Centre of the University of Indiana, USA, with appropriate ethical approval from the local Ethics Committee. Soft tissues were removed and thoroughly cleaned at this facility. Each tooth was immediately placed in a solution of distilled water and 0.1% thymol to keep them hydrated and free from bacteria. The occlusal surfaces of all teeth were gently brushed using water only.

4.2.2 Description of the implemented methods

Visual examinations

A relevant area of interest on the occlusal surface with a suspected lesion was selected for each tooth by two dentists (J. G. and R. E.) and was used as the target of investigation for all the methods compared in this study. All the samples were scored using the criteria shown in Table 4.1 for ICDAS and FOTI.

The ICDAS inspection consisted of an initial visual examination of the wet

Table 4.1: ICDAS, FOTI and Radiography scoring criteria.

Score	ICDAS	FOTI	Radiography
0	Sound	No shadow or stained area	No radiolucency
1	First visual change in enamel	Lesion stays the same width/Thin grey shadow into enamel	Radiolucency in outer half of the enamel
2	Distinct visual change in enamel	Wide grey shadow into enamel	Radiolucency in inner half of the enamel up to the EDJ
3	Localised enamel breakdown	Wide grey shadow into enamel with no evidence of dentine shadow	Radiolucency limited to the outer third of dentine
4	Underlying dentin shadow	Orange/brown or bluish/black shadow	third Radiolucency reaching the middle third of dentine or beyond

surface of the sample, a five second drying and a visual examination of the dry surface. A WHO probe was used for gentle probing when necessary. No magnification was used and the inspection was performed under ambient light. On a different session, an inspection procedure was performed with the aid of the FOTI method, consisting of placing a 0.5 mm-diameter fibre illumination probe perpendicular to the buccal and lingual surfaces, manually scanned along the surface. The FOTI system was based on a fibre-delivered illumination source (Schott Fibre Optics, Doncaster, UK) with a halogen lamp (150 W) connected to the optical fibre to bring the light to the tip of the dental probe. Note that the images of transilluminated teeth using this

technique shown in this article were not used for scoring and are shown for illustration purposes only. The investigated sites were scored by a trained and calibrated ICDAS examiner (J. G.) for ICDAS and by 2 examiners (R. E. and J. G.) for the FOTI examination. The FOTI scores were given in consensus.

Radiography

Samples were dried prior to imaging with an intra-oral X-ray system (Kodak Company, Kodak 2200) and radiographs were captured on dental films (Kodak Insight IP-21 Periapical Films F Speed) pre-labelled with an x-ray marker pen (Rontgomarker x-ray marker pen White) with a unique sample number. Radiographs were taken with the beam facing the buccal surface of the tooth using 60 kV, 7 Amp, f-value of 2 and exposure time of 0.135 ms. These are parameters that are routinely used in patients at the University Dental Hospital of Manchester and are therefore clinically relevant except for the exposure time where a 5% reduction was used from the value used in patients (0.150 ms) to compensate for the lack of radiation loss from the soft tissues (e.g. the cheek) in the in-vitro setting. Each radiograph was separately scored by two examiners (K. H. and H. P. C.)^[78] using a viewing light box (Aintree 14W C95 lamps, Dental xrayApS, UK) and a two-fold magnifying lens that eliminated ambient light. The scoring system used is as shown in Table 1. A calibration session with a set of 50 teeth was used in a calibration exercise and the inter-examiner weighted kappa value was 0.672 ± 0.133 (mean \pm std error). A consensus was sought from the two examiners in the event that the difference of the scores was more than 2 units.

Quantitative light-induced fluorescence (QLF)

A QLF system was built using a 3CCD camera (Hitachi HV-F31) with a yellow filter (Edmund Optics NT32-753, 495 nm-cut off) and a ring-illumination

consisting of 60 blue LEDs (RoithnerLasertechnik GmbH, B5-437CVD, 405 nm-emission). Occlusal images were captured. QLF images show green fluorescence corresponding to sound tissue and black areas (loss of fluorescence) otherwise. The images were scored based on a quantitative algorithm previously described[48]. This algorithm requires drawing a quadrangular mask on the images circumscribing the investigated site and seeking to place the edges of the mask only over sound enamel in order to calculate the loss of fluorescence caused by the lesion.

NIR Reflectance

A near infra-red multispectral imaging system was built using an InGaAs camera (XEVA-FPA-1.7, XenICs), with a spectral response range from 0.9 to 1.7 μm connected to a computer-controlled filter wheel with six filter positions. The filter wheel was fitted with filters in the range from 1050 nm to 1600 nm. Two broadband halogen lamps emitting visible and NIR light up to 2.5 μm (Osram 300W Halogen lamps) were used for the illumination system. The camera system and the illumination system were cross-polarised (Thorlabs NIR Linear Polarizer, 650 - 2000 nm). Images were processed in order to obtain de-noised and calibrated spectral reflectance images. Calibrated reflectance images, R , at 1050 nm, 1450 nm and 1600 nm were combined to generate a quantitative caries map, S_{caries} , obtained as described in [9].

4.2.3 Histology

Histology was used as the gold standard for this study. The individual teeth were mounted in acrylic resin blocks and hemi-sectioned through the investigation site using a 300 μm -thick diamond wheel (South Bay Technology Inc., USA). Colour photographs of the hemi-sections were captured with consistent illumination and magnification. The hemi-sections were scored to agreement by a panel of two dentists (J. G. and I. P.) taking the most severe

score of both hemi-sections for each tooth. The score criteria used was S for sound, E1 for a lesion up to the outer half of the enamel, E2 for a lesion to the inner half of the enamel, EDJ for a lesion up to the enamel-dentine junction, D1 for a lesion up to the first third of the dentine, D2 for a lesion up to the second third of the dentine and D3 for a lesion up to the pulp.

4.2.4 Statistical analysis

Optimum lesion threshold values were obtained for the quantitative optical methods (QLF and NIR) using ROC curves. Thresholds corresponding to the best Youden's index (i. e. sensitivity + specificity -1) for each histology level, this is, E1, E2, EDJ and D, were selected from the ROC curves of a training subset of 56 teeth (half of the sample population) to find the thresholds. Note that an ideal Youden's index value would be one. QLF and S_{caries} thresholds obtained with the training subset were then applied to a test subset of 56 teeth (remaining half of the sample population) to produce and report an unbiased classification analysis for an independent (test) set of data.

For completeness purposes, a second ROC analysis was performed to calculate the sensitivity and specificity using the optimum threshold values obtained by employing the whole sample set (training and test sets together) as often reported in the literature.

A three level detection analysis was implemented in all described methods in order to classify as (where Rscore below represents the radiography score):

- (a) areas with no lesion ($ICDASscore = 0$, $FOTIscore = 0$ and $Rscore = 0$, $QLFscore < th_{e-QLF}$ and $S_{caries} = 0$),
- (b) areas with enamel lesion ($1 \leq ICDASscore \leq 3$ and $1 \leq FOTIscore \leq 3$, $1 \leq Rscore \leq 2$, $0 < QLFscore < th_{d-QLF}$ and $0 < S_{caries} < th_{d-NIR}$) and
- (c) areas with dentine lesion ($ICDASscore = 4$ and $FOTIscore = 4$, $3 \leq Rscore \leq 6$, $QLFscore \geq th_{d-QLF}$ and $S_{caries} \leq th_{d-NIR}$).

Here $th_{e,technique}$ and $th_{d,technique}$ (where *technique* is QLF or NIR) correspond to the threshold values for the detection of lesions at the E1 and the D histology levels respectively and for each technique. Areas with enamel lesion include only cases with demineralisation in the outer half of the enamel (E1), the inner half of the enamel (E2) and at the enamel-dentine junction (EDJ). A confidence table was computed for the three-level classification to calculate the sensitivity and specificity against histology gold standard. This analysis was carried on for all the methods with the same sample set which is essential for a direct comparison of the techniques.

Spearman's correlation was used to investigate the relationship between the histological and the methods' scores.

4.3 Results

From histology it resulted that 23 teeth were sound, 4 had lesions in the E1, 17 in the E2 level, 22 in the EDJ and 44 had dentine lesions.

Examples of cases scored by all techniques in agreement with histology are shown in Figure 4.1, Figure 4.2 and Figure 4.3 for a sound tooth, a tooth with enamel demineralisation and a tooth with dentine demineralisation, respectively. Each figure shows the tooth colour image with a line drawn where the sectioning was made, the picture of the corresponding histological section, the radiographic image, the FOTI image (only for illustration purposes), the QLF image and the NIR S_{caries} map. The lesion classification is made at an E1 histology detection threshold ($ICDAS_{score} > 0$, $FOTI_{score} > 0$, $R_{score} > 0$, $QLF_{score} \geq 381.7$ and $NIRS_{caries} > 0$) and at a D histology detection threshold ($ICDAS_{score} \geq 4$, $FOTI_{score} \geq 4$, $R_{score} \geq 3$, $QLF \geq 2530$ and $NIRS_{caries} \geq 0.0718$). This enabled a three level grading of the lesion: a) no lesion, b) lesion up to the EDJ and c) lesion into dentine.

A three level detection threshold has been previously proposed to distinguish between sensitivity and specificity for enamel and dentin lesions[79, 75].

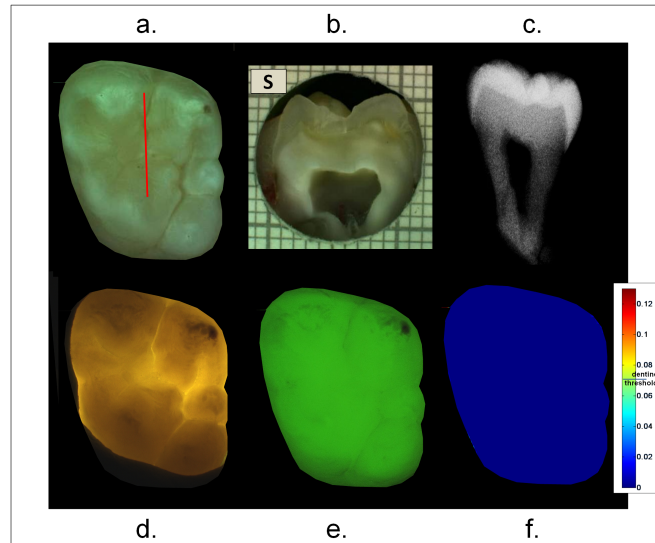


Figure 4.1: Sound tooth: tooth colour image with a line drawn where the sectioning was made (a), picture of the corresponding histological section (b), radiographic image (c), FOTI image (only for illustration purposes) (d), QLF image (e) and NIR $S_{carries}$ map (f). All the techniques scored this tooth as sound.

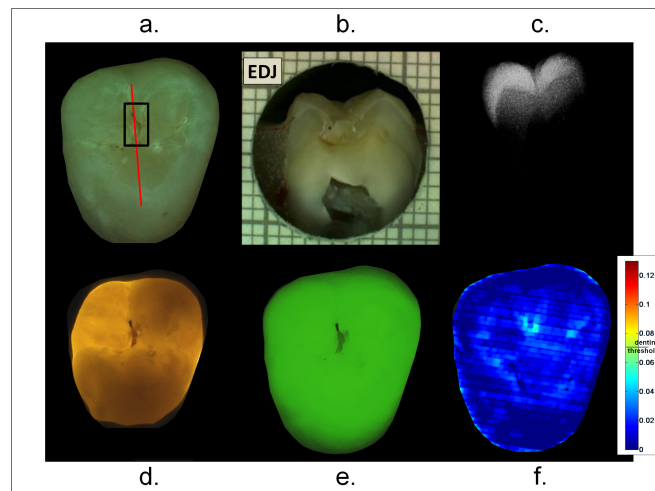


Figure 4.2: Tooth with enamel demineralisation. All the techniques scored this tooth as with a lesion in the enamel, in particular the ICDAS and FOTI scores were both 1, QLF scored it with a lesion at the E1, Radiography scored it as a 2 and NIR as with a lesion at the E2.

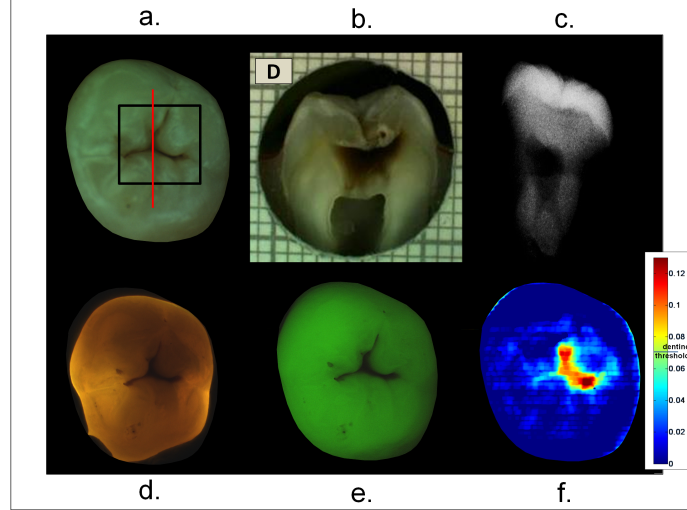


Figure 4.3: Tooth with dentine demineralisation: tooth colour image with a line drawn where the sectioning was made (a), picture of the corresponding histological section (b), radiographic image (c), FOTI image (only for illustration purposes) (d), QLF image (e) and NIR S_{caries} map (f). All the techniques scored this tooth as with a lesion in the dentine.

Table 4.2: Confidence table of the visible methods in comparison with histology at the three detection levels.

		ICDAS			FOTI		
		S	1,2,3	4	S	1,2,3	4
Histology	Sound	10	1	0	11	1	0
	E1, E2, EDJ	0	22	0	3	19	0
	Dentine	0	10	13	0	10	13

Table 4.3: Confidence table of QLF, Radiography and NIR methods in comparison with histology at the three detection levels.

		QLF			Radiography			NIR		
		S	E1-EDJ	D	S	1,2	3-5	S	1,2,3	4
Histology	Sound	7	2	2	9	1	1	8	3	0
	E1, E2, EDJ	5	13	4	13	3	6	4	8	10
	Dentine	0	1	21	3	0	19	0	4	19

A confidence table of lesion classification for each technique against histology is shown in Tables 4.2 and 4.3 and Tables 4.4 and 4.5 for the *test* and the *whole* sample sets. The resulting sensitivities and specificities for both

Table 4.4: Table of the results of visual methods in comparison with histology.

		ICDAS					FOTI				
whole set		S	1	2	3	4	S	1	2	3	4
Histology	Sound	20	3	0	0	0	22	1	0	0	0
	E1	0	2	1	1	0	1	2	0	1	0
	E2	0	11	6	0	0	2	11	4	0	0
	EDJ	0	10	9	3	0	1	12	7	2	0
	Dentine	0	1	5	14	24	0	1	7	9	26

Table 4.5: Table of the results of QLF, Radiography and NIR methods in comparison with histology.

		QLF					Radiography					NIR				
whole set		S	E1	E2	EDJ	D	S	1	2	3	4-5	S	1	2	3	4
Histology	Sound	16	0	2	1	4	15	2	3	3	0	19	1	3	0	0
	E1	2	1	0	1	0	4	0	0	0	0	2	0	2	0	0
	E2	3	1	10	0	3	13	1	1	2	0	2	0	8	1	6
	EDJ	1	2	8	2	9	12	0	4	4	2	2	0	6	3	11
	Dentine	0	0	0	1	43	5	0	0	24	3	1	0	4	0	39

the *test* and the *whole* sample sets are shown in Tables 4.6 and 4.7 for each technique. Note that *whole* sample set data analysis is commonly reported in the literature where no distinction is made between *test* and *training* sets; this can result in a biased analysis but was included for completeness.

Maximum accuracy would correspond to an area under the ROC curve equal to unity; Table 4.8 shows the values obtained for QLF and NIR S_{caries} and these ranged from 0.87 to 0.92 for QLF and from 0.90 to 0.94 for NIR S_{caries} .

Spearman's correlation coefficients between histology and each of the methods evaluated are shown in Table 4.9.

Table 4.6: Table of values of sensitivity and specificity at the three detection levels for visual methods.

Test set	Visual inspection			
	<i>ICDAS</i>		<i>FOTI</i>	
	Sensitivity	Specificity	Sensitivity	Specificity
Sound	90%	> 99%	> 99%	93%
Enamel	> 99%	67%	86%	70%
Dentine	56%	> 99%	56%	> 99%
Whole set	Sensitivity	Specificity	Sensitivity	Specificity
Sound	87%	> 99%	96%	95%
Enamel	> 99%	66%	91%	72%
Dentine	54%	> 99%	59%	> 99%

Table 4.7: Table of values of sensitivity and specificity at the three detection levels for QLF, Radiography and NIR methods.

Test set	<i>Radiography</i>		<i>QLF</i>		<i>NIR Reflectance</i>	
	Sensitivity	Specificity	Sensitivity	Specificity	Sensitivity	Specificity
Sound	81%	63%	63%	88%	73%	91%
Enamel	13%	97%	59%	90%	36%	79%
Dentine	86%	78%	95%	81%	83%	70%
Whole set	Sensitivity	Specificity	Sensitivity	Specificity	Sensitivity	Specificity
Sound	65%	61%	69%	93%	96%	84%
Enamel	14%	92%	72%	83%	58%	88%
Dentine	89%	83%	87%	89%	77%	89%

Table 4.8: Table of values of areas under the ROC curve at all the detection levels calculated on the training set for the methods requiring ROC analysis, namely QLF and NIR.

Areas under ROC curves	QLF	NIR
E1	0.89	0.93
E2	0.92	0.94
EDJ	0.87	0.91
D	0.88	0.90

Table 4.9: Table of values of Spearman’s correlation at all the detection levels for all the methods.

Spearman’s correlations	ICDAS	FOTI	Radiography	QLF	NIR
Histology	0.885 **	0.882 **	0.647 **	0.733 **	0.774 **

**Correlation is significant at the 0.01 level (2-tailed).

4.4 Discussion

As shown in Tables 4.6 and 4.7, the NIR method registered a sensitivity (and specificity) to detect disease in either enamel or dentine of 91% (and 73%) compared to 88% (and 63%) for QLF and 63% (and 81%) for radiography; however this was superseded by ICDAS and FOTI which yielded sensitivity (and specificity) of > 99% (and 90%) and 93% (and > 99%), respectively. These values resulted from the application to the *test* sample set of the thresholds calculated on the *training* sample set. Applying the optimum thresholds obtained for the quantitative methods (QLF and NIR) to the *training* sample set used to calculate the thresholds themselves can result in a self-fulfilling bias in the analysis; we have, therefore, presented the outcomes for the *whole* sample set in Tables 4.6 and 4.7 purely for completeness as this is the most commonly reported method in the literature.

A three-level detection analysis was performed not only in order to distinguish cases that were sound from cases affected by caries but also to accurately investigate true enamel lesion detection sensitivity and specificity and true dentine lesion detection sensitivity and specificity.

Note that the detection of lesions that would favour preventive approaches is emphasised in this study, reducing the occurrences of unnecessarily invasive treatment. According to the International Caries Classification and Management System (ICCMS)[80, 2], ICDAS score 3 reflects microcavitation but is not considered as an obvious decay; therefore, this would not necessarily warrant surgical intervention and is classified as enamel lesion for the comparative purposes of this study in the three-level detection described above.

Note that the samples were gently brushed with soft bristled toothbrushes prior to measurement. This could result in a cleaner surface and consequently a possible false positive lesion detection reduction for ICDAS, FOTI and QLF. Moreover, conducting an in-vitro visual inspection with ICDAS and FOTI might result in an enhanced visibility of lesions not normally faced intra-orally.

ICDAS was used as a non-destructive method to select samples from sound to advanced lesions in the attempt to achieve equal distribution of lesions with varying lesion depth. From the selection it resulted that 20 teeth were sound, 27 were scored as ICDAS 1, 21 ICDAS 2, 18 ICDAS 3, 24 ICDAS 4. However, from histology it resulted that only 4 had lesions in the E1. We found that most of the cases that were scored as ICDAS 1 revealed to have lesions at the EDJ level once examined by histology. This limited the amount of cases with a lesion at the E1 level and can be a possible explanation for the reduced sensitivity registered by the NIR technique at the enamel level. It was found that the NIR detection sensitivity at this level was only higher than radiography's, as shown in Table 4.7. In particular, the NIR method scored two of the four E1 cases as having lesions at the E2 level and the other two as sound. Moreover, two from these cases were scored as ICDAS 1 while the remaining two were scored as ICDAS 2 and ICDAS 3. This was similarly observed using FOTI. QLF correctly scored one case while scoring two as having lesions at the E2 level and one at the EDJ level. Radiography scored all four cases as sound.

At the dentine level, the NIR method yielded similar outcomes for dentine lesions sensitivity (and specificity) as radiography did, as seen in Table 4.7; QLF showed the highest detection sensitivity. This is surprising as QLF relies on the collagen matrix in dentine as a fluorescence emission source when quantifying enamel lesions and is normally not recommended for advanced lesions. There are two possible explanations for this observation; either the QLF method correctly registers a high loss of fluorescence when

there is collagen breakdown in a dentine lesion or it rather registers the stain that is commonly present when there is a dentine lesion. Note that the lowest dentine lesion sensitivity was equally observed for both visual inspection methods; however both had the highest specificities.

A limitation of QLF when compared to the NIR method is that an area circumscribing the suspected lesion on the occlusal side of the tooth needs to be drawn by a trained user. This results in an average score, which is not location-specific. Moreover, if the tooth is suspected sound, the whole occlusal surface is normally included in the analysis. Extreme care had to be taken in order to ensure that the edges of the area drawn would only include sound enamel; however, this sometimes can include several lesions and the score possibly would not reflect the precise severity of the lesion in question. An example of this is shown in Figure 4.4, where the whole fissure had to be included. This is unlike the NIR mapping as it can be used to score the precise location of interest corresponding to the histology section.

The NIR method relies on the amount of light back-scattered from the tooth surface as an indication of lesion severity, such as in porous enamel tissue, and on the light absorption by the water accumulated inside the lesion, such as in cavitated dentine tissue. Therefore, a highly porous but shallow enamel lesion may result in a score that could be as high as in a tooth with a deeper but less porous enamel lesion due to water accumulation or pooling. This can explain cases of over-scoring by the NIR method when compared to histology, as in the example shown in Figure 4.5.

The NIR S_{caries} scored it as having a dentinal lesion while the histological section showed the lesion was at the enamel-dentine junction. Therefore, severity of mineral loss might be more closely related to scattering than depth; however, this would require further investigation. Note that the tooth in Figure 4.5 is characterised by heavy stain, disguising for the visual methods the fact that the lesion has reached the EDJ. For the same reason, QLF over-scored the tooth as demineralised in the dentine. Radiography scored

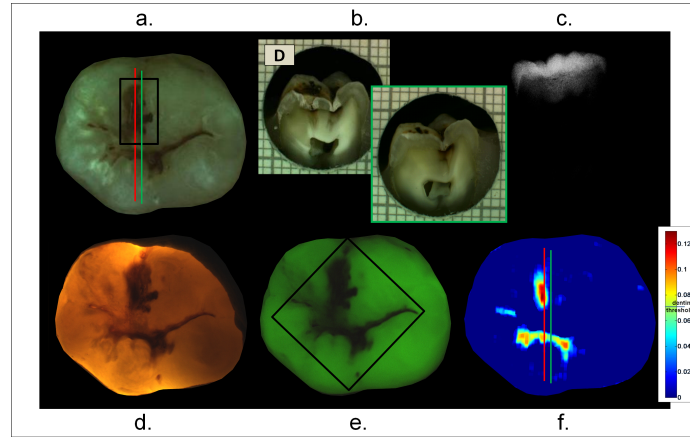


Figure 4.4: Tooth colour image with a line drawn where the sectioning was made (a), picture of the corresponding histological section (b), radiographic image (c), FOTI image (only for illustration purposes) (d), QLF image (e) and NIR S_{caries} map (f). The user-defined patch the QLF algorithm needs to calculate fluorescence loss has to circumscribe the suspected lesion with the sides superimposing areas the user supposes to be sound, as shown in (e). In cases like this, QLF cannot be location-specific, resulting in an average score of the whole tooth. Selecting a smaller area would mean drawing the patch over brown areas and getting wrong score values.

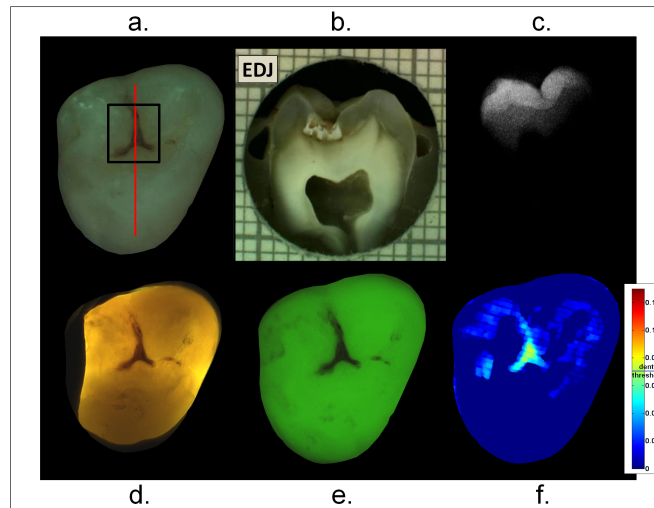


Figure 4.5: Case of NIR S_{caries} over-scoring. The NIR S_{caries} scored it as having dentinal lesion because of highly porous enamel lesion increasing the NIR signal due to water absorption.

it as 2, detecting presence of lesion in the EDJ.

On the other hand, an excess of enamel surface moisture can also result in scattering attenuation and therefore under-scoring. Due to the variation in sample anatomy, the drying protocol could have been more effective at removing the surface moisture in some teeth than others. An under-scored case is shown in Figure 4.6.

The water absorption at the lesion indicated by the red line does not show

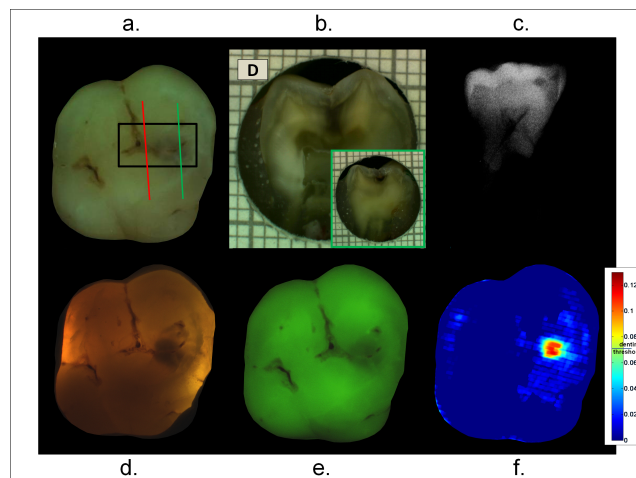


Figure 4.6: Case of NIR $S_{carries}$ under-scoring: tooth colour image with a line drawn where the sectioning was made (a), picture of the corresponding histological section (b), radiographic image (c), FOTI image (only for illustration purposes) (d), QLF image (e) and NIR $S_{carries}$ map (f). For the NIR $S_{carries}$ in the case of the red cut the amount of water detected, spread in the tissue and not concentrated in a specific reservoir, was not sufficient to score a deeper lesion. The method correctly detected the lesion below the intact enamel surface indicated by the green line.

to be concentrated in a specific reservoir but rather distributed in the porous surface of the affected tissue. In this case the amount of water detected was not sufficient to detect a deeper lesion. Note, however, that the hidden lesion below the intact enamel surface in this same case, indicated by the green line (corresponding to the histological section in the green frame), was adequately detected by the NIR method.

All the methods compared in this study are affected by stain except radiography and NIR. Radiography is, however, considered as an invasive technique due to the emission of ionising radiation. Moreover, occlusal lesion assessment from bitewings radiography is complex as the nature of the measurement results in a superposition of the overall buccal-to-lingual tooth surface x-ray absorption from the teeth. Figure 4.4 shows an example of a tooth severely affected by stain. In this case both the visual methods, ICDAS and FOTI, incorrectly under-scored the tooth underneath the stain patch. This is a good example of how the stain over a carious lesion made the loss of fluorescence from caries undistinguishable for QLF. Although radiography, similarly to NIR, has scored this tooth correctly, it provides no occlusal view. Moreover, comparing the consecutive histology section, identified by the green line and the green frame, the NIR S_{caries} shows the distinction between stained sound sites and stained demineralisation. Note that the stain pattern is not reproduced by the NIR image which further supports the absent effect of stain on these measurements as previously reported[79].

Note that the surface appears intact above the underlying dentinal lesion. ICDAS and FOTI under-scored this lesion. Radiography was clearly in agreement with histology presenting a shadow in dentine. The QLF correctly detected the lesion in dentine but only at the fissure missing the extension of the spread. The NIR S_{caries} was able to both detect the lesion in the dentine and to map its extension; it has correctly scored the lesion both under sound and demineralised enamel.

Further studies are required to understand the effect of fluorosis on early demineralisation detection. Sound teeth with mild fluorosis can affect the threshold at the E1 level. Figure 4.7 shows an example of a tooth affected by fluorosis. This tooth was scored as sound by histology; although the NIR S_{caries} map did not show the fluorosis pattern, it scored this tooth with an E1 demineralisation at the area of interest and E2 as maximum in the whole map.

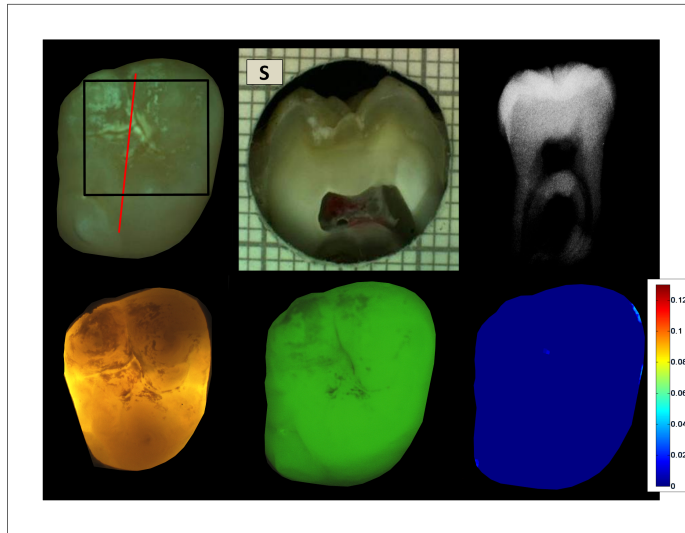


Figure 4.7: Tooth affected by fluorosis. The NIR S_{caries} map does not show the fluorosis pattern, it scored this tooth with an E1 demineralisation at the area of interest and E2 as maximum in the whole map.

Figure 4.8 shows an example of a tooth with enamel breakdown at the area of interest.

Table 4.10 shows a summary of the different characteristics of the caries detection methods explored.

The visual methods require training, are subjective and have a coarse sensitivity, for instance the ICDAS system does not have a clear distinction among E2, EDJ and mid-dentine lesions. Visual inspection, radiography and QLF only yield a single score for the whole tooth and do not provide spatial information on its health status. QLF does not allow lesion mapping and although it is an imaging technique, it still relies on an experienced user with knowledge of sound and unhealthy fluorescence areas to draw a mask around the suspected lesion and generate a score.

Previous studies on occlusal caries comparing the performances of visual examination and other diagnostic tools showed a good agreement with this study. A review by Zandon et al.[15] considered the performance of early

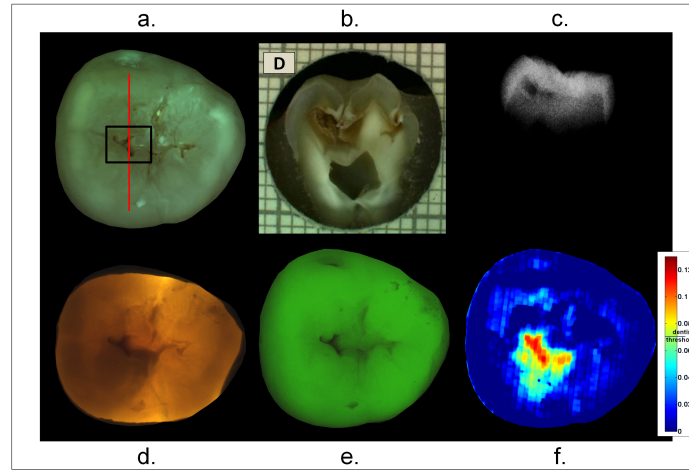


Figure 4.8: Case of lesion NIR S_{caries} and Radiography are able to detect while other methods fail: tooth colour image with a line drawn where the sectioning was made (a), histological section (b), radiographic image (c), FOTI image (d), QLF image (e) and NIR S_{caries} map (f). Here the surface appears intact above the underlying dentinal lesion extension: ICDAS and FOTI under-scored it while QLF detected only the lesion at the fissure with no fluorescence loss shown where the lesion extends.

Table 4.10: Table of the properties the techniques have. Desirable features in green, unwanted ones in red.

Properties	ICDAS	FOTI	Radiography	QLF	NIR
Non-invasive	✓	✓		✓	✓
Occlusal Imaging				✓	✓
Map of lesions					✓
Objective without user input needed					✓
Objective but user input needed				✓	
Pre-knowledge required				✓	
Training required	✓	✓	✓		
Overall score	✓	✓	✓	✓	
Stain sensitive	✓	✓		✓	

caries detection tools available in the literature, including QLF, ECM, IR laser fluorescence and FOTI. For instance, for QLF they reported occlusal lesion sensitivity and specificity of 0.61 ± 0.14 and 0.59 ± 0.18 (*mean \pm std.deviation*) respectively considering selected studies. In the present study the equivalent sensitivity and specificity was found to be 0.93 and 0.69, considering as lesion scores greater or equal to the histological E1 level on the *whole* sample set. The authors indicated concerns about the confounding effect of stain on the determination of the lesion depth and the operator influence on the performance of all the methods investigated, where a different operator may obtain different results. A previous *in-vitro* study with FOTI[35] reported a sensitivity and specificity of 0.96 and 0.74 to occlusal lesion detection, respectively. The corresponding values in this study were 0.95 and 0.96, respectively using the whole sample set for lesions more severe or equal to the enamel level. A sensitivity of 0.89 and a specificity of 0.92 to detect dentine lesions were reported by the same authors whereas in this study the equivalent values were > 0.99 and 0.59 respectively. Authors recommended the use of FOTI along with visual inspection as a tool for enhancing dentine lesion detection, where the visual method is less effective; however, the extensive training required and the influence of stain on the performances of all methods involved in the study were the main downfalls reported for these techniques.

This comparative study allowed for revealing advantages and disadvantages of the considered methods. This is the first study comparing visual techniques, such as ICDAS and FOTI, and imaging techniques, such as radiography and QLF, with a novel imaging technique, the NIR reflectance technique, especially focusing on how its unique features can support the clinician activities along with the systems already in use.

4.5 Conclusions

In this study 110 teeth were examined with common techniques used in the clinics and in the research field, namely ICDAS, FOTI, Radiography and QLF. Examining the same set of teeth with a NIR multispectral reflectance imaging system allowed for a direct comparison of the methods against this novel technique. The features that could enhance the detection success of the NIR imaging method were also highlighted.

Results of sensitivity and specificity showed that the NIR technique can be particularly useful for the discrimination between sound and demineralised tissue, and show a performance as good as radiography at detecting dentine lesions.

It is demonstrated that this technique can overcome issues faced by visual inspection and visible-light based detection techniques since it is not affected by stain. Moreover it is non-ionising which renders it more suitable for routine inspection than radiographs. The ability to image, quantify and map the lesions on the occlusal surface make this tool attractive for supporting clinical decision-making, monitoring dental caries lesions and enhanced patient communication.

Chapter 5

Conclusions

5.1 Summary and conclusions

The aim of the research presented in this thesis was to validate a novel noninvasive technique, NIR multi-spectral reflectance imaging, for caries detection, including the design and implementation of the instrument as well as the comparison of its performance against other caries detection methods.

Advantages of this technique rely on the optical property of dental tissues in the near infrared spectral region. At visible wavelength the main limit for caries detection is sound enamel light scattering, obstructing access to see any lesion within the enamel thickness and the dentine. This makes visual inspection mainly useful for superficial evident lesions or severe caries. It is known that sound enamel scattering coefficient decreases with increasing wavelength and that sound enamel attenuation coefficient in the NIR range is 1-2 orders of magnitude less than in the visible range. This means that NIR light can penetrate the tissue 1-2 orders more than visible wavelengths. Enamel becomes transparent in the NIR[70]. Moreover, stain, very often present on dental surfaces and main confounding factor for dentists during clinical inspection, does not absorb NIR light. Stain affects the majority of tools and techniques for caries detection but it does not appear in NIR

images.

There are significant advantages also comparing NIR reflectance to other techniques, such as Radiography or other NIR techniques. The NIR reflectance imaging technique gives an alternative view to radiographs and this is useful for occlusal caries detection, for which radiographs are not adequate but when lesions affect the tooth in depth and surgical treatment may be already required. Moreover, it does not emit any ionising radiation, making it safe in case of frequent examinations also on young patients and in pregnancy. Despite their relevant utility in the diagnosis of approximal caries lesions and other oral diseases, radiographs for caries detection are also affected by a high assessment inter-observer variability, making them a very subjective diagnostic tool.

The main innovation on other NIR detection methods is that NIR reflectance combines more wavelengths with the aim of punctually (at pixel level) mapping the occlusal view of the tooth with information on degree of lesion severity. Moreover, the combination of wavelengths gives the opportunity to be free of any user input. Other methods, such as NIR transillumination, are less effective at detecting early lesion[34] and still requires it for quantification of image contrast, which can be considered related to lesion severity but it is a score limited to the area selected by the user. Contrast is also dependent on distance of the investigated lesion from the light source due to heterogeneous illumination and from sound areas during user selection.

From the comparison of the NIR reflectance technique with conventional detection methods, such as visual inspection using ICDAS scoring system, visual inspection with the aid of FOTI, radiography and QLF, on 110 extracted teeth occlusal lesions, it resulted that visual inspection methods recorded the highest values of sensitivity (ICDAS: >99%, FOTI: 93%) and specificity to dental caries (FOTI: >99%, ICDAS: 90%). However, these methods could have been highly facilitated by the in-vitro viewing of the samples since light

and sight were not obstructed by the surrounding oral mucosa and gingiva. Sensitivity to dental caries was higher for NIR (91%) than for QLF (88%) and radiography (63%) while specificity was higher for radiography (81%) than for NIR (73%) and QLF (63%). This study highlighted that visual methods are a good first screening step especially for selecting whether a tooth needs further examination. But they are affected by high intra- and inter-variability as well as radiography. Radiography is an indispensable diagnostic tool for hard-tissue oral disease screening and to detect approximal caries but frequent recourse to radiographs and the current dose of ionising radiations emitted by the common intraoral and extraoral imaging techniques using x-rays need reconsideration[60]. QLF is a very interesting method because it gives a lesion score but also an occlusal image of the fluorescence of the tooth. This is not a map of lesions though, but it gives a visual feeling of the tooth health and the possibility to store and compare images. In this study QLF performed similarly to NIR reflectance but it is affected by some limitations, mainly due to the use of fluorescence in the visible spectrum, undergoing the same issues as visible inspection, such as highly sensitivity to the confounding effects of stain. Moreover, it needs for user input since the lesion area to investigate has to be selected in a way that is dependent on the anatomy of each tooth and its lesion degree in the caries process, thus involving user training, knowledge and experience. For lesion activity monitoring, the same selected area may become inconvenient in time making lesions at different times not comparable.

When looking at the results focusing only at the enamel level, visual inspection methods (sensitivity, ICDAS: >99%, FOTI: 86%; specificity, ICDAS: 67%, FOTI: 70%) are very sensitive but not very specific, meaning they tend to score teeth with dentine lesions as with enamel lesions. Sound enamel scattering blocks the diagnostic ability and limits it to the enamel. Among the non-visible methods, radiography had a very low sensitivity (sensitivity, 13%; specificity, 97%) as expected; QLF (sensitivity, 59%; specificity, 90%)

had a lower sensitivity than visible methods but performed better than radiography and NIR (sensitivity, 36%; specificity, 79%). The limited amount of cases with early demineralisation did not allow for a wider analysis of the NIR response to those lesions. But it is not easy to get extracted early demineralised teeth. Moreover, at the EDJ level many lesions were scored as dentine lesions, demonstrating this method is able to discriminate a severe lesion but not necessary the depth of the lesion. Often, though, severity may correspond to depth, due to the natural caries propagation process, developing vertically in enamel and creating cavities in dentine.

When looking at the results focusing at the dentine level, it becomes clear how visual inspection methods (sensitivity, ICDAS: 56%, FOTI: 56%; specificity, ICDAS: >99%, FOTI: >99%) lack of detection ability in depth and a further aid from other techniques is needed. The NIR reflectance detection ability (sensitivity, 83%; specificity, 70%) was lower than radiography (sensitivity, 86%; specificity, 78%) but comparable and lower than QLF (sensitivity, 95%; specificity, 81%). The lower values of sensitivity and specificity could be still explained by the indirect relation of the NIR score to lesion depth. Despite this three-level detection analysis appeared to be the fairest, especially for comparison of such different techniques, it does not fully represent the meaning of the NIR score. The NIR reflectance method measures scattering from the enamel and water absorption. While increase of scattering is due to increase of porosity in the NIR transparent enamel, water absorption can be measured at any level of the dental tissue, with no distinction between enamel and dentine. The measurement procedure tried to take into account and limit this effect by air-drying for 15 seconds at approximately 5 cm to remove moisture from the enamel surface. But in fact it is not possible to remove the water in the enamel thickness, unless the tooth has a thin enamel layer. Therefore, on one hand, a severe lesion in enamel, with presence of water, might not be distinguished from the signal coming from presence of water in dentine. In the same way, a severe lesion in enamel

but with elevated degree of porosity increases the detected scattering. This value could also be as high as what was classified as dentine lesion in this study. On the other hand, lesions at the EDJ or first third of dentine that are covered by intact enamel tissue and are porous but are not water *reservoir*, may be classified as enamel lesions. Most frequently these cases do not need operative treatment though, falling within those conditions requiring preventive attentions, as it would be for cases classified as enamel lesions in this study.

This novel imaging technique was implemented, validated and compared with other detection methods during this study. It was shown that it is able to detect and quantify dental caries even in presence of stained occlusal surfaces, easily confounded as demineralised by visual inspection, ICDAS and FOTI, and QLF. Moreover, NIR reflectance help visualising lesion areas but also objectively quantify the lesions at pixel precision on the whole occlusal surface. It also provides an alternative view (occlusal) to radiography without ionising radiation. This method can be an adjunct to clinical detection for the ability to detect dental caries when other methods fail, assist in the decision making process and aid monitoring of preventive interventions; it can enhance patient communication and in some cases avoid the use of radiographs.

5.2 Future work

There are several possible directions for future work based upon the investigations presented in this thesis. Developments both from the clinical point of view and from the technical one, as expected by a discipline applying technology to medicine, are desirable.

Clinically, the next natural step would be the investigation of NIR reflectance performances on smooth surfaces in-vivo. Incisors may be imaged and examination methodology may consist of bitewing-like images for de-

tection of approximal lesions. From the above considerations, sound enamel would be expected to be transparent to the NIR, instead demineralisation would be scattered, becoming evident. For this kind of examination, it may result that one of the wavelengths detecting mainly scattering would be enough to discriminate early approximal caries, as long as only enamel is interested.

Mild fluorosis is a confounding factor that tends to be diagnosed as early lesion. It would be interesting to study a pool of teeth affected by mild fluorosis to see whether the image analysis shown in this thesis would be able to reduce or threshold this condition off of the NIR images. As it was for NIR transillumination, the use of one wavelength may not be enough for obtaining fluorosis-free results[67].

Another fundamental test for this technique would be a study on reproducibility, calculating scoring variability, if recorded. This method was designed for being human error independent as much as possible, from the set-up use through the methodology and the image analysis until the lesion map output. Of course, it would be interesting to test whether environmental light and temperature changes provoke a response variation.

From the technical point of view, the development of a NIR reflectance intra-oral probe is definitely the main target. During the studies for this thesis, a big attention and considerable efforts were put at designing, building and implementing a method based on NIR reflectance that used LED light sources at the wavelengths selected by the studies described in this thesis. The aim of the LED experiment was to check if LED source could replace halogen white light in the NIR reflectance method set-up.

5.2.1 LED experiment

Roithner LaserTechnik high power LED array with 60 chips were used for this experiment. The aim of this study was to find an alternative illumination source to broadband halogen lamps for future miniaturisation of the instrument and development of a NIR intraoral probe. The choice for LED

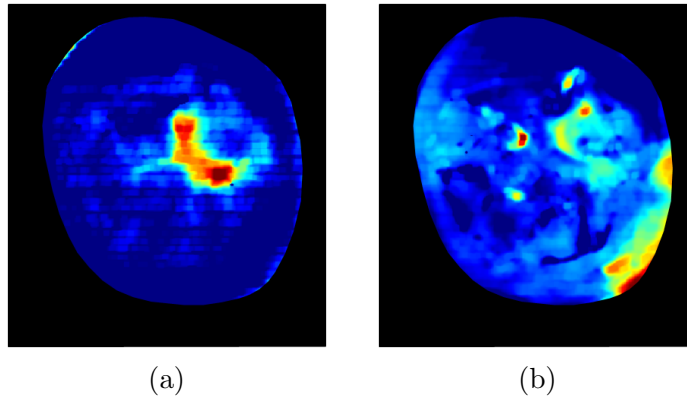


Figure 5.1: Comparison between NIR reflectance lesion map with a) broad-band source and filters and b) LED light sources.

illumination was due to a great waste of lamp power considering that only three wavelengths were needed and filtered out of such a wide range of wavelengths. The main concern, though, was for the amount of power needed in order for the sample to be fully illuminated. This is the reason for testing high power LEDs: at 1050 nm (peak wavelength) and 120 mW optical output power; at 1450 nm and 60 mW power; and at 1550 nm and 60 mW power. Their bandwidth was ± 50 nm.

This study validated the NIR reflectance imaging technique using LEDs as illumination system against histological reference standard. The wavelengths used were 1050, 1450 and 1550 nm, that were the LED wavelengths available on the market as much close as possible to the validated wavelengths. A total of 112 extracted teeth were examined. For each tooth, occlusal surface images at the different wavelengths were captured and then combined to generate the NIR quantitative lesion map.

A visual comparison of the LED result and the broadband light result is shown Figures 5.1a and 5.1b. Example of LED images are presented in Figures 5.2a, 5.2b and 5.2c. A significant correlation (Spearman's coefficient = 0.531, $p < 0.01$) between this NIR caries score and the histological score has been found, with detection sensitivity of 72% and specificity 64% for sound

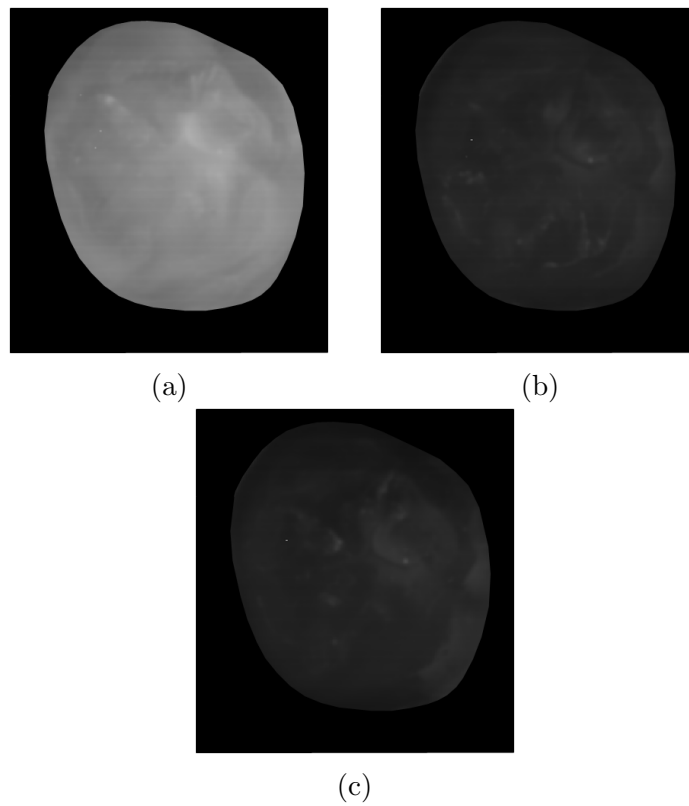


Figure 5.2: LED NIR reflectance images: a) 1050 nm, b) 1450 nm and c) 1550 nm

areas, 18% sensitivity and 97% specificity for lesions on the enamel and 69% sensitivity and 67% specificity for lesions at the dentine, with ROC curves applied to training set and results got from test set.

Unfortunately the difference in reflectance between Figures 5.2b and 5.2c is minimal and mainly due to polariser leakage, which caused specular reflections to appear in the images. These were different for each LED due to the different light direction, as the three LED lights were distributed around the tooth. The LED at 1450 and 1550 nm do not have a narrow wavelength bandwidth and thus it became impossible to distinguish the two wavelengths since their bandwidths overlap.

5.2.2 Imaging fiber optic experiment

Another experiment with the aim of studying possible solutions for the best way to design a hand-held intraoral probe was the one using an imaging optical fiber. Apart from studying how to deliver light to the probe, the transmission of the image to the detector was also analysed. For the wavelengths required by the NIR reflectance algorithm it is difficult to find fiber bundles able to transmit signal especially at 1450 and 1550 nm. The experiment was carried out testing two different fiber bundles: the first one was a Schott wound image bundle with a bend radius of 51 mm and 10 microns fiber size in 4x4 mm fiber end format. This bundle is made of many fibers tightened together; the second one was made of 100 ± 10 thousands number of pixels, it was not flexible though. From the specifications their transmittance performance at the required wavelengths was unclear, and in particular for the former bundle this was the first test of transmittance in the NIR. The results were poor. In the first case the connections among fibers inside the bundle were visible, producing noise on the image; moreover, only the image at 1050 nm was visible. The second bundle could transmit the three images, as shown in Figure 5.3. A pool of 15 teeth were used for testing the new element. LED light was used and, as a note of remark, an extension tube

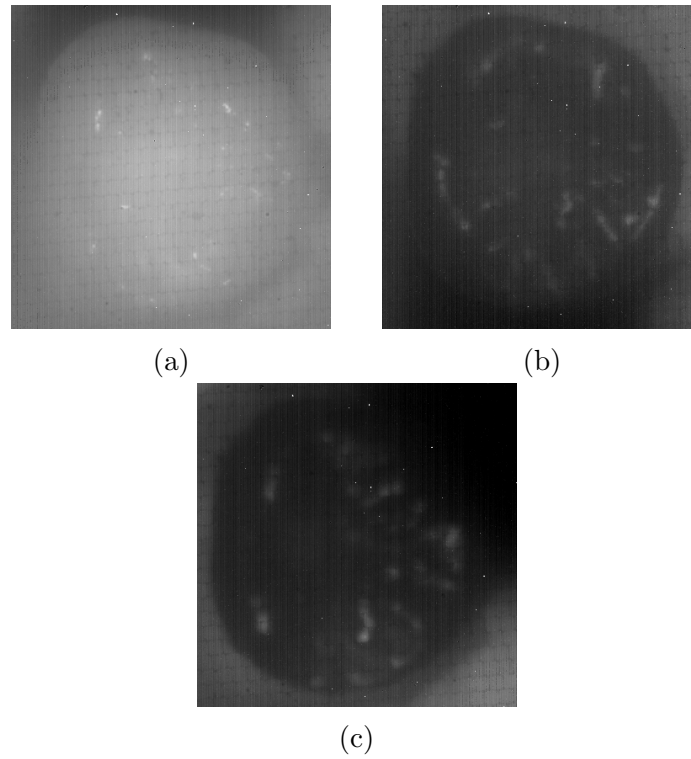


Figure 5.3: LED NIR reflectance images with imaging fiber bundle: a) 1050 nm, b) 1450 nm and c) 1550 nm

of ~ 13.5 cm was required in order to increase the magnification spoiling the depth of focus. So the images resulted blurred and a rigorous analysis was not achieved.

Bibliography

- [1] Jan Kühnisch, Sofia Tranæs us, Birgit Angmar-Mänsson, and Lutz Stöß er. Quantitative light-induced fluorescence measurement a future method for the dentist? *53(2)*:131–141, 2002.
- [2] Poul Erik Petersen. The World Oral Health Report 2003 - WHO Global Oral Health Programme. Technical report, World Health Organization, Geneva, 2003.
- [3] N Pitts, B Amaechi, R Niederman, A-M Acevedo, R Vianna, C Ganss, A Ismail, and E Honkala. Global oral health inequalities: dental caries task group–research agenda. *Advances in dental research*, 23(2):211–20, May 2011.
- [4] Domenick T Zero. Dentifrices, mouthwashes, and remineralization/caries arrestment strategies. *BMC Oral Health*, 6(S9):1–13, January 2006.
- [5] P Bottenberg, D N J Ricketts, C Van Loveren, C Rahiotis, and A G Schulte. Decision-making and preventive non-surgical therapy in the context of a European Core Curriculum in Cariology. *European Journal of Dental Education*, 15(Suppl 1):32–39, November 2011.
- [6] E.A.M. Kidd and O. Fejerskov. What Constitutes Dental Caries? Histopathology of Carious Enamel and Dentin Related to the Action

- of Cariogenic Biofilms. *Journal of Dental Research*, 83(suppl 1):C35–C38, July 2004.
- [7] P Anderson, J Beeley, P Manarte Monteiro, H de Soet, S Andrian, B Amaechi, and M-C D N J M Huysmans. A European Core Curriculum in Cariology: the knowledge base. *European Journal of Dental Education*, 15(Suppl 1):18–22, November 2011.
- [8] Iain A Pretty. Caries detection and diagnosis: novel technologies. *Journal of Dentistry*, 34(10):727–39, November 2006.
- [9] Christian Zakian, Iain Pretty, and Roger Ellwood. Near-infrared hyperspectral imaging of teeth for dental caries detection. *Journal of Biomedical Optics*, 14(6):064047–7, 2009.
- [10] N B Pitts. Are we ready to move from operative to non-operative/preventive treatment of dental caries in clinical practice? *Caries research*, 38(3):294–304, 2004.
- [11] B Nyvad and O Fejerskov. Assessing the stage of caries lesion activity on the basis of clinical and microbiological examination. *Community Dentistry and Oral Epidemiology*, 25(1):69–75, February 1997.
- [12] B Nyvad, V Machiulskiene, and V Baelum. Reliability of a new caries diagnostic system differentiating between active and inactive caries lesions. *Caries research*, 33(4):252–60, 1999.
- [13] B. Nyvad, V. Machiulskiene, and V. Baelum. Construct and Predictive Validity of Clinical Caries Diagnostic Criteria Assessing Lesion Activity. *Journal of Dental Research*, 82(2):117–122, February 2003.
- [14] A Wenzel, E H Verdonschot, G J Truin, and K G König. Accuracy of visual inspection, fiber-optic transillumination, and various radiographic image modalities for the detection of occlusal caries in extracted non-cavitated teeth. *Journal of Dental Research*, 71(12):1934–7, 1992.

-
- [15] Andréa Ferreira Zandoná and Domenick T Zero. Diagnostic tools for early caries detection. *Journal of the American Dental Association (1939)*, 137(12):1675–84, December 2006.
- [16] Amid I Ismail, W Sohn, M Tellez, A Amaya, A Sen, H Hasson, and N B Pitts. The International Caries Detection and Assessment System (ICDAS): an integrated system for measuring dental caries. *Community Dentistry and Oral Epidemiology*, 35(3):170–178, 2007.
- [17] A Jablonski-Momeni, V Stachniss, D N Ricketts, M Heinzl-Gutenbrunner, and K Pieper. Reproducibility and accuracy of the ICDAS-II for detection of occlusal caries in vitro. *Caries Research*, 42(2):79–87, January 2008.
- [18] D F Côrtes, K R Ekstrand, A R Elias-Boneta, and R P Ellwood. An in vitro comparison of the ability of fibre-optic transillumination, visual inspection and radiographs to detect occlusal caries and evaluate lesion depth. *Caries Research*, 34(6):443–7, 2000.
- [19] V. Machiulskiene, B. Nyvad, and V. Baelum. A Comparison of Clinical and Radiographic Caries Diagnoses in Posterior Teeth of 12YearOld Lithuanian Children. *Caries Research*, 33(5):340–348, 1999.
- [20] D N Ricketts, E A Kidd, B G Smith, and R F Wilson. Clinical and radiographic diagnosis of occlusal caries: a study in vitro. *Journal of Oral Rehabilitation*, 22(1):15–20, January 1995.
- [21] A Schneiderman, M Elbaum, T Shultz, S Keem, M Greenebaum, and J Driller. Assessment of dental caries with Digital Imaging Fiber-Optic Transillumination (DIFOTI): in vitro study. *Caries Research*, 31(2):103–10, January 1997.

- [22] C. Longbottom and M.-C.D.N.J.M. Huysmans. Electrical Measurements for Use in Caries Clinical Trials. *Journal of Dental Research*, 83(Suppl 1):C76–C79, July 2004.
- [23] Y L Fennis-Ie, E H Verdonschot, and M A van't Hof. Performance of some diagnostic systems in the prediction of occlusal caries in permanent molars in 6- and 11-year-old children. *Journal of Dentistry*, 26(5-6):403–8, 1998.
- [24] Hanna M Alwas-Danowska, Alphons J M Plasschaert, Stanislaw Suliborski, and Emiel H Verdonschot. Reliability and validity issues of laser fluorescence measurements in occlusal caries diagnosis. *Journal of Dentistry*, 30(4):129–34, May 2002.
- [25] X Q Shi, S Tranaeus, and B Angmar-Månsson. Validation of DIAGNOdent for quantification of smooth-surface caries: an in vitro study. *Acta Odontologica Scandinavica*, 59(2):74–8, April 2001.
- [26] Bennett T Amaechi and Susan M Higham. Quantitative light-induced fluorescence: a potential tool for general dental assessment. *Journal of Biomedical Optics*, 7(1):7–13, January 2002.
- [27] B. Angmar-Mansson and J. J. ten Bosch. Quantitative light-induced fluorescence (QLF): a method for assessment of incipient caries lesions. *Dentomaxillofacial Radiology*, 30(6):298–307, November 2001.
- [28] Robert Jones, Daniel Fried, and San Francisco. Attenuation of 1310-nm and 1550-nm laser light through sound dental enamel. *Lasers in Dentistry VIII, Proc. SPIE*, 4610:187–190, 2002.
- [29] Cynthia L Darling, Gigi D Huynh, and Daniel Fried. Light scattering properties of natural and artificially demineralized dental enamel at 1310 nm. *Journal of Biomedical Optics*, 11(3):34023–11, 2006.

- [30] Robert Jones, Gigi Huynh, Graham Jones, and Daniel Fried. Near-infrared transillumination at 1310-nm for the imaging of early dental decay. *Optics express*, 11(18):2259–65, September 2003.
- [31] B W Colston, M J Everett, L B Da Silva, L L Otis, P Stroeve, and H Nathel. Imaging of hard- and soft-tissue structure in the oral cavity by optical coherence tomography. *Applied Optics*, 37(16):3582–5, June 1998.
- [32] Bennett T Amaechi, Adrian Podoleanu, Susan M Higham, and David A Jackson. Correlation of quantitative light-induced fluorescence and optical coherence tomography applied for detection and quantification of early dental caries. *Journal of Biomedical Optics*, 8(4):642–7, October 2003.
- [33] M C D N J M Huysmans, H P Chew, and R P Ellwood. Clinical studies of dental erosion and erosive wear. *Caries Research*, 45(Suppl 1):60–68, January 2011.
- [34] J Wu and D Fried. High contrast near-infrared polarized reflectance images of demineralization on tooth buccal and occlusal surfaces at $\lambda = 1310\text{-nm}$. *Lasers in Surgery and Medicine*, 41(3):208–13, March 2009.
- [35] D F Côrtes, R P Ellwood, and K R Ekstrand. An in vitro comparison of a combined FOTI/visual examination of occlusal caries with other caries diagnostic methods and the effect of stain on their diagnostic performance. *Caries Research*, 37(1):8–16, 2003.
- [36] K. R. Ekstrand, S. Martignon, D. J. N. Ricketts, and V. Qvist. Detection and Activity Assessment of Primary Coronal Caries Lesions: A Methodologic Study. *Operative Dentistry*, 32(3):225–235, June 2007.
- [37] Amid I Ismail, Woosung Sohn, Marisol Tellez, Jenefer M Willem, James Betz, and James Lepkowski. Risk indicators for dental caries using the

- International Caries Detection and Assessment System (ICDAS). *Community Dentistry and Oral Epidemiology*, 36(1):55–68, February 2008.
- [38] Km Shivakumar, Sumanth Prasad, and Gn Chandu. International Caries Detection and Assessment System: A new paradigm in detection of dental caries. *Journal of conservative dentistry*, 12(1):10–6, January 2009.
- [39] D Banting, H Eggertsson, K R Ekstrand, C Longbottom, E Reich, D Ricketts, R Selwitz, W Sohn, D Zero, Amid I Ismail, and Restorative Sciences. Rationale and Evidence for the International Caries Detection and Assessment System (ICDAS II). (September 2005):1–43, 2012.
- [40] Sofia Tranaeus, Xie-Qi Shi, and Birgit Angmar-Månsson. Caries risk assessment: methods available to clinicians for caries detection. *Community Dentistry and Oral Epidemiology*, 33(4):265–73, August 2005.
- [41] K W Neuhaus, R Ellwood, A Lussi, and N B Pitts. Traditional lesion detection aids. *Monographs in Oral Science*, 21:42–51, January 2009.
- [42] Antonio Carlos Pereira, Hafsteinn Eggertsson, Esperanza Angeles Martinez-Mier, Fábio Luiz Mialhe, George Joseph Eckert, and Domenick Thomas Zero. Validity of caries detection on occlusal surfaces and treatment decisions based on results from multiple caries-detection methods. *European Journal of Oral Sciences*, 117(1):51–7, February 2009.
- [43] C.M. Mitropoulos. The Use of Fibre-Optic Transillumination in the Diagnosis of Posterior Approximal Caries in Clinical Trials. *Caries Research*, 19(4):379–384, 1985.
- [44] H Hintze, A Wenzel, B Danielsen, and B Nyvad. Reliability of visual examination, fibre-optic transillumination, and bite-wing radiography,

- and reproducibility of direct visual examination following tooth separation for the identification of cavitated carious lesions in contacting approximal surfaces. *Caries Research*, 32(3):204–9, January 1998.
- [45] H Bjelkhagen, F Sundström, B Angmar-Månsson, and H Rydén. Early detection of enamel caries by the luminescence excited by visible laser light. *Swedish dental journal*, 6(1):1–7, January 1982.
- [46] A Thylstrup, S A Leach, and V Qvist. Optical properties of dentin. In *Dentine and dentine reactions in the oral cavity*, chapter 3, pages 34–40. Oxford University Press, 1987.
- [47] B Angmar-Månsson and J J ten Bosch. Quantitative light-induced fluorescence (QLF): a method for assessment of incipient caries lesions. *Dento maxillo facial radiology*, 30(6):298–307, November 2001.
- [48] E de Josselin de Jong, F Sundström, H Westerling, S Tranaeus, J J ten Bosch, and B Angmar-Månsson. A new method for in vivo quantification of changes in initial enamel caries with laser fluorescence. *Caries research*, 29(1):2–7, January 1995.
- [49] R Hibst and R Gall. Development of a Diode Laser-Based Fluorescence Caries Detector. *Caries Research*, 32:294, 1998.
- [50] Raimund Hibst and Robert Paulus. A new approach on fluorescence spectroscopy for caries detection. *SPIE Conference on Lasers in Dentistry V*, 3593:141–147, 1999.
- [51] Raimund Hibst and Robert Paulus. Caries Detection by Red Excited Fluorescence: Investigations on Fluorophores. *Caries Research*, 33:295, 1999.
- [52] Raimund Hibst and Robert Paulus. Molecular Basis of Red Excited Caries Fluorescence. *Caries Research*, 34:323, 2000.

-
- [53] X Q Shi, S Tranæ us, and B Angmar-Må nsson. Comparison of QLF and DIAGNOdent for quantification of smooth surface caries. *Caries research*, 35(1):21–6, 2001.
- [54] K C Huth, K W Neuhaus, M Gygax, K Bücher, a Crispin, E Paschos, R Hickel, and a Lussi. Clinical performance of a new laser fluorescence device for detection of occlusal caries lesions in permanent molars. *Journal of dentistry*, 36(12):1033–40, December 2008.
- [55] E A Kidd, M N Naylor, and R F Wilson. Prevalence of clinically undetected and untreated molar occlusal dentine caries in adolescents on the Isle of Wight. *Caries research*, 26(5):397–401, January 1992.
- [56] K L Weerheijm, H J Groen, A J Bast, J A Kieft, M A Eijkman, and W E van Amerongen. Clinically undetected occlusal dentine caries: a radiographic comparison. *Caries research*, 26(4):305–9, January 1992.
- [57] K L Weerheijm. Occlusal 'hidden caries'. *Dental update*, 24(5):182–4, June 1997.
- [58] Michele Baffi Diniz, Jonas Almeida Rodrigues, Klaus W Neuhaus, Rita C L Cordeiro, and Adrian Lussi. Influence of examiner's clinical experience on the reproducibility and accuracy of radiographic examination in detecting occlusal caries. *Clinical Oral Investigations*, 14(5):515–23, October 2010.
- [59] I Espelid, A B Tveit, and A Fjelltveit. Variations among dentists in radiographic detection of occlusal caries. *Caries research*, 28(3):169–75, January 1994.
- [60] John B Ludlow, Laura E Davies-ludlow, and Stuart C White. Patient risk related to common dental radiographic examinations: The impact

- of 2007 International Commission on Radiological Protection recommendations regarding dose calculation. *American Dental Association*, 139(9):1237–1243, 2008.
- [61] Bart Vandenberghe, Reinhilde Jacobs, and Hilde Bosmans. Modern dental imaging: a review of the current technology and clinical applications in dental practice. *European Radiology*, 20(11):2637–55, November 2010.
- [62] M C D N J M Huysmans, J Kühnisch, and J J ten Bosch. Reproducibility of electrical caries measurements: a technical problem? *Caries research*, 39(5):403–10, 2005.
- [63] J.J. Ten Bosch, Y. Fennis-le, and E.H. Verdonschot. Time-dependent Decrease and Seasonal Variation of the Porosity of Recently Erupted Sound Dental Enamel in vivo. *Journal of Dental Research*, 79(8):1556–1559, August 2000.
- [64] J Wang, S Sakuma, A Yoshihama, S Kobayashi, and H Miyazaki. An Evaluation and Comparison of Visual Inspection, Electrical Caries Monitor and Caries Detector Dye Methods in Detecting Early Occlusal Caries in Vitro Study. *Journal of Dental Health*, 50(2):223–230, 2000.
- [65] Christopher Bühler, Patara Ngaotheppitak, and Daniel Fried. Imaging of occlusal dental caries (decay) with near-IR light at 1310-nm. *Optics express*, 13(2):573–82, January 2005.
- [66] Chulsung Lee, Cynthia L. Darling, and Daniel Fried. In vitro near-infrared imaging of occlusal dental caries using germanium-enhanced CMOS camera. *Proceedings of SPIE*, 7549:75490K–75490K–7, 2010.
- [67] Krista Hirasuna, Daniel Fried, and Cynthia L Darling. Near-infrared imaging of developmental defects in dental enamel. *Journal of Biomedical Optics*, 13(4):044011, 2011.

- [68] Daniel Fried, John Xie, Sahar Shafi, John D B Featherstone, Thomas M Breunig, and Charles Le. Imaging caries lesions and lesion progression with polarization sensitive optical coherence tomography. *Journal of Biomedical Optics*, 7(4):618–27, October 2002.
- [69] You-Chen Tao, Kenneth Fan, and Daniel Fried. Near-infrared image-guided laser ablation of artificial caries lesions. *Proceedings of SPIE*, 6425:64250T–64250T–8, 2007.
- [70] Michal Staninec, Shane M Douglas, Cynthia L Darling, Kenneth Chan, Hobin Kang, Robert C Lee, and Daniel Fried. Non-destructive clinical assessment of occlusal caries lesions using near-IR imaging methods. *Lasers in Surgery and Medicine*, on line(September), November 2011.
- [71] Anahita Jablonski-Momeni, David N J Ricketts, Vitus Stachniss, Regina Maschka, Monika Heinzl-Gutenbrunner, and Klaus Pieper. Occlusal caries: Evaluation of direct microscopy versus digital imaging used for two histological classification systems. *Journal of Dentistry*, 37(3):204–11, March 2009.
- [72] Negin Mosahebi and David Nigel James Ricketts. Effect of contact media on the diagnostic quality of electrical resistance measurements for occlusal caries. *Community Dentistry and Oral Epidemiology*, 30(3):161–7, June 2002.
- [73] Dustin Lee, Daniel Fried, and Cynthia L. Darling. Near-IR multi-modal imaging of natural occlusal lesions. *Proceedings of SPIE*, 7162:71620X–71620X–7, 2009.
- [74] M.-C.D.N.J.M. Huysmans and C. Longbottom. The Challenges of Validating Diagnostic Methods and Selecting Appropriate Gold Standards. *Journal of Dental Research*, 83(1):C48–C52, July 2004.

-
- [75] C M Zakian, A M Taylor, R P Ellwood, and I A Pretty. Occlusal caries detection by using thermal imaging. *Journal of Dentistry*, 38(10):788–95, October 2010.
- [76] Soojeong Chung, Daniel Fried, Michal Staninec, and Cynthia L Darling. Multispectral near-IR reflectance and transillumination imaging of teeth. *Biomedical Optics Express*, 2(10):2804–14, October 2011.
- [77] Christopher M. Buehler and Daniel Fried. Near-IR imaging of occlusal dental decay. *Proceedings of SPIE*, 5687:125–131, 2005.
- [78] Keith Horner, John Rout, and Vivian E. Rushton. *Interpreting Dental Radiographs (Quintessentials of Dental Practice)*. Quintessence Pub Co, 1 edition, 2002.
- [79] Silvia Salsone, Andrew Taylor, Juliana Gomez, Iain Pretty, Roger Ellwood, Mark Dickinson, Giuseppe Lombardo, and Christian Zakian. Histological validation of near-infrared reflectance multispectral imaging technique for caries detection and quantification multispectral imaging technique for caries detection. *Journal of Biomedical Optics*, 17(7):076009–1–10, 2012.
- [80] International Caries Detection and Assessment System Coordinating Committee. International Caries Detection and Assessment System (ICDAS II) Criteria Manual. Technical report, ICDAS Coordinating Committee, 2009.